JHEP

Published for SISSA by Springer

Received: April 11, 2015
Revised: May 15, 2015
Accepted: May 27, 2015
Published: June 16, 2015

QCD effects on direct detection of wino dark matter

Junji Hisano,[a,b,c] **Koji Ishiwata**[d] **and Natsumi Nagata**[c,e]

[a] *Kobayashi-Maskawa Institute for the Origin of Particles and the Universe, Nagoya University, Nagoya 464-8602, Japan*

[b] *Department of Physics, Nagoya University, Nagoya 464-8602, Japan*

[c] *Kavli IPMU (WPI), UTIAS, University of Tokyo, Kashiwa, Chiba 277-8584, Japan*

[d] *Institute for Theoretical Physics, Kanazawa University, Kanazawa 920-1192, Japan*

[e] *William I. Fine Theoretical Physics Institute, School of Physics and Astronomy, University of Minnesota, Minneapolis, MN 55455, U.S.A.*

E-mail: hisano@eken.phys.nagoya-u.ac.jp, ishiwata@hep.s.kanazawa-u.ac.jp, nagat006@umn.edu

Abstract: We complete the calculation of the wino-nucleon scattering cross section up to the next-to-leading order in α_s. We assume that the other sparticles are decoupled and wino interacts with the Standard Model particles via the weak interaction. As a result, the uncertainties coming from the perturbative QCD are significantly reduced to be smaller than those from the nucleon matrix elements. The resultant scattering cross section is found to be larger than the leading-order one by about 70%, which is well above the neutrino background. In the limit of large wino mass the spin-independent scattering cross section with proton turns out $\sigma^p_{\rm SI} = 2.3\ ^{+0.2}_{-0.3}\ ^{+0.5}_{-0.4} \times 10^{-47}$ cm^2 (errors come from perturbative calculation and input parameters, respectively). The computation for a generic SU(2)$_L$ multiplet dark matter is also presented.

Keywords: NLO Computations, Supersymmetry Phenomenology

ArXiv ePrint: 1504.00915

doi:10.1007/JHEP06(2015)097

JHEP06(2015)097

Contents

JHEP06(2015)097

1 Introduction

Weakly-interacting massive particles (WIMPs) are promising candidates for dark matter (DM) in the Universe. Many theoretical models beyond the Standard Model predict WIMPs and it is known that the thermal WIMP scenario can explain the present energy density of dark matter in those models. The early stage of the experiments at the Large Hadron Collider, however, has found no evidence for new physics near the electroweak scale so far. In particular, the experiments give severe bounds on new colored particles, such as gluino and squarks in the supersymmetric (SUSY) models [1, 2]. This situation may imply that most of the new particles in the high energy theory have masses much larger than the electroweak scale and only a WIMP, probably accompanied with some non-colored particles, is accessible in the TeV-scale experiments.

The current experimental consequences would fit in with a simple SUSY breaking scenario. If the SUSY breaking is induced by non-singlet chiral superfields (as is often

the case with the dynamical SUSY breaking [3–8]), gaugino masses are induced by the anomaly mediation mechanism [9, 10] and thus suppressed by a loop factor compared with the gravitino mass. A generic Kähler potential gives masses of the order of the gravitino mass to scalar particles and higgsino. In this framework, the neutral wino is found to be the lightest SUSY particle and thus becomes a candidate for dark matter in the Universe. Actually, its thermal relic abundance explains the observed energy density of DM if the wino DM has a mass of 2.7–3.1 TeV [11]. For relatively light wino DM, on the other hand, the non-thermal production via the late time decay of gravitino could be invoked to provide the correct abundance of DM [12, 13]. As this scenario [10, 14–18] requires the SUSY breaking scale to be much higher than the electroweak scale, a relatively heavy mass for the Higgs boson is predicted [19–28], which is consistent with the observed value $m_h \simeq 125\,\text{GeV}$ [29, 30]. Although such a high SUSY-breaking scale requires a severe fine-tuninig to realize the electroweak scale, it is phenomenologically desirable since it relaxes the SUSY flavor and CP problems [31–37], the dimension-five proton decay problem [38–42], and some cosmological problems [43–45]. Gauge coupling unification is found to be still preserved with good accuracy [46]. For these reasons, the wino DM scenario attracts a lot of attention, and its phenomenology has been studied widely.

A lot of efforts have been dedicated to searching for the wino DM. A robust constraint is provided by the Large Hadron Collider experiment; charged winos with a mass of 270 GeV or less have been excluded at 95% C.L. [47]. For prospects of the wino search in future collider experiments, see ref. [48–54]. On the other hand, signal of the wino DM may be detected in cosmic ray observations. Since the wino DM has large annihilation cross section [55, 56], cosmic rays from annihilating winos are promising tools to detect the wino DM indirectly. The mass of wino DM, M, is excluded as $M \leq 320$ GeV and 2.25 TeV $\leq M \leq 2.43$ TeV at 95% C.L. [57] by using gamma ray data from dwarf spheroidal galaxies provided by Fermi-LAT collaboration [58]. See also ref. [59] for relevant discussion. Gamma rays from the Galactic center provided by the H.E.S.S. [60] may give a strong limit on the wino DM, though the consequences are quite dependent on the DM density profile used in the analysis [61–63]. Developments in both theory [64–68] and observation enable us to probe a wide range of mass region of the wino DM in future indirect detection experiments.

Direct detection of dark matter is another important experiment to study the nature of dark matter. Currently the most stringent limits are provided by the LUX experiment [69]; it sets an upper limit on the spin-independent (SI) WIMP-nucleon elastic scattering cross section as $\sigma_{\text{SI}} < 7.6 \times 10^{-46}\ \text{cm}^2$ at a WIMP mass of 33 GeV. Moreover, various future projects with ton-scale detectors are now ongoing and expected to have significantly improved sensitivities. To test the wino DM scenario in the direct detection experiments, one needs to evaluate the wino-nucleon scattering cross section precisely, with the theoretical uncertainties being sufficiently controlled. This scattering is induced by loop diagrams if the higgsino and squarks are much heavier than wino [70]. At present, the leading order (LO) calculation for the scattering cross section is given in the literature [71–74]; in these works, the SI scattering cross section with a nucleon is evaluated as $\sigma_{\text{SI}} \sim 10^{-47}\ \text{cm}^2$. For other relevant works, see refs. [75–82]. Since the predicted scattering rate of the wino DM is larger than those of the neutrino backgrounds [83], one expects that the future

JHEP06(2015)097

direct detection experiments may eventually catch a signal of the wino DM. However, it was pointed out by the authors of refs. [79, 80, 82] that the present calculation may suffer from large uncertainties. They further found that these uncertainties mainly come from the neglect of the higher order contribution in perturbation theory, not from the error of the nucleon matrix elements, which may alter the SI cross section by a factor. To reduce the uncertainties, therefore, we need to go beyond the LO calculation.

In this paper, we complete this calculation up to the next-to-leading order (NLO) in the strong coupling constant α_s. For this purpose, we first reformulate the computation based on the effective theoretical approach. The relevant interactions are expressed in terms of the effective operators, whose Wilson coefficients are given up to the NLO with respect to α_s. The coefficients are evolved down to the scale at which the nucleon matrix elements of the effective operators are evaluated, by means of the renormalization group equations (RGEs). This procedure allows us to include the NLO QCD effects systematically.

The rest of the paper is organized as follows. In the next section, we describe the formulation mentioned above. All of the matching conditions as well as the RGEs are presented here. Then, in section 3, we show our results for the SI scattering cross section and discuss the uncertainties of the calculation. In section 4, we also present the results for a generic $\mathrm{SU}(2)_L$ multiplet DM. Those who are interested in a quick reference may find our results in these two sections. Section 5 is devoted to conclusion and discussion.

2 Formalism

In this section, we give a formalism to evaluate the SI scattering cross section of the wino DM with a nucleon. We will carry out the calculation up to the NLO in the strong coupling constant α_s. The formalism given here is based on the method of effective field theories, which consists of the following three steps. Firstly, we obtain the effective operators at the electroweak scale $\mu_W \simeq m_Z$ (m_Z is the mass of the Z boson) by integrating out heavy particles whose masses are not less than the electroweak scale. This step is carried out in terms of the operator product expansions (OPEs). Secondly, we evolve the Wilson coefficients of the effective operators using the RGEs down to the scale at which the nucleon matrix elements of the operators are evaluated. Finally, we express the SI effective coupling of a wino DM with a nucleon in terms of the Wilson coefficients and the nucleon matrix elements. From this effective coupling, one readily obtains the SI scattering cross section.

2.1 Effective Lagrangian

First let us formulate the effective Lagrangian which gives rise to the SI interactions of the wino DM with quarks and gluon. The effective Lagrangian comprises two types of the higher dimension operators — the scalar and the twist-2 type operators — as follows [84]:

$$\mathcal{L}_{\mathrm{eff}} = \sum_{i=q,G} C^i_{\mathrm{S}} \mathcal{O}^i_{\mathrm{S}} + \sum_{i=q,G} \left(C^i_{\mathrm{T}_1} \mathcal{O}^i_{\mathrm{T}_1} + C^i_{\mathrm{T}_2} \mathcal{O}^i_{\mathrm{T}_2} \right), \tag{2.1}$$

JHEP06(2015)097

Proton		Neutron	
$f_{T_u}^{(p)}$	0.019(5)	$f_{T_u}^{(n)}$	0.013(3)
$f_{T_d}^{(p)}$	0.027(6)	$f_{T_d}^{(n)}$	0.040(9)
$f_{T_s}^{(p)}$	0.009(22)	$f_{T_s}^{(n)}$	0.009(22)

Table 1. Mass fractions computed with the lattice simulations of QCD [89, 90].

with

$$\begin{aligned}
\mathcal{O}_{\rm S}^{q} &\equiv m_q \bar{\chi}^0 \chi^0 \bar{q} q \,, \\
\mathcal{O}_{\rm S}^{G} &\equiv \frac{\alpha_s}{\pi} \bar{\chi}^0 \chi^0 G^a_{\mu\nu} G^{a\mu\nu} \,, \\
\mathcal{O}_{\rm T_1}^{i} &\equiv \frac{1}{M} \bar{\chi}^0 i\partial^\mu \gamma^\nu \chi^0 \mathcal{O}^i_{\mu\nu} \,, \\
\mathcal{O}_{\rm T_2}^{i} &\equiv \frac{1}{M^2} \bar{\chi}^0 (i\partial^\mu)(i\partial^\nu) \chi^0 \mathcal{O}^i_{\mu\nu} \,,
\end{aligned} \tag{2.2}$$

Here χ^0, q, and $G^a_{\mu\nu}$ denote the wino DM, quarks, and the field strength tensor of gluon field, respectively; m_q are the masses of quarks; M is the mass of the wino DM; $\mathcal{O}^q_{\mu\nu}$ and $\mathcal{O}^G_{\mu\nu}$ are the twist-2 operators of quarks and gluon, respectively, which are defined by[1]

$$\begin{aligned}
\mathcal{O}^q_{\mu\nu} &\equiv \frac{1}{2} \bar{q} i \left(D_\mu \gamma_\nu + D_\nu \gamma_\mu - \frac{1}{2} g_{\mu\nu} \not{D} \right) q \,, \\
\mathcal{O}^G_{\mu\nu} &\equiv G^{a\rho}_\mu G^a_{\nu\rho} - \frac{1}{4} g_{\mu\nu} G^a_{\rho\sigma} G^{a\rho\sigma} \,,
\end{aligned} \tag{2.3}$$

with D_μ the covariant derivative. Here we neglect the operators that are suppressed in the non-relativistic limit. We have performed the quark mass/momentum expansion and kept only the LO terms. Factors of $1/M$ and $1/M^2$ in the definition of $\mathcal{O}^i_{T_1}$ and $\mathcal{O}^i_{T_2}$, respectively, compensate the derivatives on the DM fields, whose time component reduces to the DM mass in the non-relativistic limit. Moreover, we have used the equations of motion to eliminate redundant operators [86, 87]. These effective operators are renormalized at the electroweak scale $\mu_W \simeq m_Z$ with $N_f = 5$ active quarks ($q = u, d, s, c, b$). The Wilson coefficients of the operators are to be determined below. Notice that we have included the strong coupling constant α_s/π in the definition of the gluon scalar-type operator $\mathcal{O}^G_{\rm S}$ [88]. We will discuss the validity in the next subsection.

2.2 Nucleon matrix elements

In order to compute the scattering cross section of the wino DM with a nucleon, we need the nucleon matrix elements of the scalar and twist-2 type quark and gluon operators presented above. Since these two types of the operators do not mix with each other under the renormalization group (RG) flow, it is possible to consider these two types separately.

[1] We have changed the definition of $\mathcal{O}^G_{\mu\nu}$ by a factor of -1 from those in refs. [71–73, 84]. We follows the conversion in ref. [85].

JHEP06(2015)097

$g(2)$	0.464(2)		
$u(2)$	0.223(3)	$\bar{u}(2)$	0.036(2)
$d(2)$	0.118(3)	$\bar{d}(2)$	0.037(3)
$s(2)$	0.0258(4)	$\bar{s}(2)$	0.0258(4)
$c(2)$	0.0187(2)	$\bar{c}(2)$	0.0187(2)
$b(2)$	0.0117(1)	$\bar{b}(2)$	0.0117(1)

Table 2. Second moments of the PDFs of proton evaluated at $\mu = m_Z$. We use the CJ12 next-to-leading order PDFs given by the CTEQ-Jefferson Lab collaboration [92].

For the scalar-type quark operators, we use the results from the QCD lattice simulations. The values of the mass fractions of a nucleon $N(= p, n)$, which are defined by

$$f_{T_q}^{(N)} \equiv \langle N | m_q \bar{q} q | N \rangle / m_N \,, \tag{2.4}$$

are shown in table 1. Here m_N is the nucleon mass. They are taken from ref. [74], which are computed with the recent results of the lattice QCD simulations [89, 90].

The nucleon matrix element of $\mathcal{O}_{\rm S}^G$, on the other hand, is evaluated by means of the trace anomaly of the energy-momentum tensor in QCD [91]:

$$\Theta^\mu{}_\mu = \frac{\beta(\alpha_s)}{4\alpha_s} G^a_{\mu\nu} G^{a\mu\nu} + (1 - \gamma_m) \sum_q m_q \bar{q} q \,. \tag{2.5}$$

Here the beta-function $\beta(\alpha_s)$ and the anomalous dimension γ_m are defined by the following equations:

$$\beta(\alpha_s) \equiv \mu \frac{d\alpha_s}{d\mu} \,, \qquad \gamma_m m_q \equiv \mu \frac{dm_q}{d\mu} \,, \tag{2.6}$$

whose explicit forms will be given in eqs. (2.37) and (2.38), respectively. By putting the operator (2.5) between the nucleon states at rest, we obtain

$$\langle N | \frac{\alpha_s}{\pi} G^a_{\mu\nu} G^{a\mu\nu} | N \rangle = m_N \frac{4\alpha_s^2}{\pi \beta(\alpha_s; N_f = 3)} \left[1 - (1 - \gamma_m) \sum_q f_{T_q}^{(N)} \right] . \tag{2.7}$$

This formula is obtained with $N_f = 3$ quark flavors. Notice that the relation (2.5) is an operator equation and thus scale-invariant. This is because the energy-momentum tensor is corresponding to the current of the four momentums, which is a physical quantity and thus not renormalized. As a consequence, eq. (2.7) should hold at any scales. We will evaluate the matrix element at the hadronic scale $\mu_{\rm had} \simeq 1$ GeV in the following calculation.

Since $\beta(\alpha_s) = \mathcal{O}(\alpha_s^2)$, the r.h.s. of eq. (2.7) have a size of $\mathcal{O}(m_N)$. Namely, although we include a factor of α_s/π in the definition of $\mathcal{O}_{\rm S}^G$, its nucleon matrix element is not suppressed by the factor. It should be also noted that the scalar-type quark operator $m_q \bar{q} q$ is scale-invariant to all orders in perturbation theory (in a mass-independent renormalization scheme) and then the matrix element of $\mathcal{O}_{\rm S}^G$ is independent of the scale at the LO in α_s. This is another reason for our definition of $\mathcal{O}_{\rm S}^G$.

JHEP06(2015)097

Finally, the nucleon matrix elements of the twist-2 operators are given by the second moments of the parton distribution functions (PDFs):

$$\langle N(p)|\mathcal{O}^q_{\mu\nu}|N(p)\rangle = m_N\Big(\frac{p_\mu p_\nu}{m_N^2} - \frac{1}{4}g_{\mu\nu}\Big)(q^{(N)}(2;\mu) + \bar{q}^{(N)}(2;\mu))\,, \tag{2.8}$$

$$\langle N(p)|\mathcal{O}^G_{\mu\nu}|N(p)\rangle = -m_N\Big(\frac{p_\mu p_\nu}{m_N^2} - \frac{1}{4}g_{\mu\nu}\Big)g^{(N)}(2;\mu)\ . \tag{2.9}$$

with

$$q^{(N)}(2;\mu) = \int_0^1 dx\ x\ q^{(N)}(x,\mu)\,, \tag{2.10}$$

$$\bar{q}^{(N)}(2;\mu) = \int_0^1 dx\ x\ \bar{q}^{(N)}(x,\mu)\,, \tag{2.11}$$

$$g^{(N)}(2;\mu) = \int_0^1 dx\ x\ g^{(N)}(x,\mu)\ . \tag{2.12}$$

Here $q^{(N)}(x,\mu)$, $\bar{q}^{(N)}(x,\mu)$ and $g^{(N)}(x,\mu)$ are the PDFs of quark, antiquark and gluon in nucleon at the scale μ, respectively. Contrary to the case of the scalar matrix elements, we have the values of the PDFs at various scales. In table 2, for example, we present the second moments at the scale of $\mu = m_Z$. Here we use the CJ12 next-to-leading order PDFs given by the CTEQ-Jefferson Lab collaboration [92]. It turns out that with the definition of the gluon twist-2 tensor given in eq. (2.3), the second moment for gluon $g(2)$ is of the same order of magnitude as those for quarks so that the r.h.s. of eqs. (2.8) and (2.9) are $\mathcal{O}(m_N)$. This justifies the definition (2.2), where we do not include a factor of α_s/π in the definition of $\mathcal{O}^G_{\mathrm{T}_1}$ and $\mathcal{O}^G_{\mathrm{T}_2}$. Our definition for the gluon operators ($\mathcal{O}^G_{\mathrm{S}}$, $\mathcal{O}^G_{\mathrm{T}_1}$, and $\mathcal{O}^G_{\mathrm{T}_2}$) clarifies the order counting with respect to α_s/π [88].

2.3 Wilson coefficients

Now we evaluate the Wilson coefficients of the effective operators at the electroweak scale μ_W to the NLO in α_s/π. We use the $\overline{\mathrm{MS}}$ scheme in the following calculation. The scattering of a pure neutral wino χ^0 with a nucleon is induced via the weak interactions accompanied by the charged winos $\chi^\pm$. The interaction Lagrangian is given by

$$\mathcal{L}_{\mathrm{int}} = g_2\overline{\chi^0}\not{W}\chi^+ + \mathrm{h.c.}\,, \tag{2.13}$$

where g_2 and W_μ are the $\mathrm{SU}(2)_L$ gauge coupling constant and the W boson, respectively. Since the winos do not couple to the Higgs field directly and the mass difference ΔM between the neutral and charged winos is radiatively generated after the electroweak symmetry breaking, ΔM is much smaller than the DM mass itself or other masses which enter into our computation; according to the recent NLO computation given in ref. [93], $\Delta M \simeq 165\,\mathrm{MeV}$. Therefore, we safely neglect it in the following discussion.

Before looking into the details of the calculation, we first summarize the procedure of the computation as well as the approximations we have used in the calculation. In figure 1, we show the diagrams which induce the couplings of wino DM with quarks and

JHEP06(2015)097

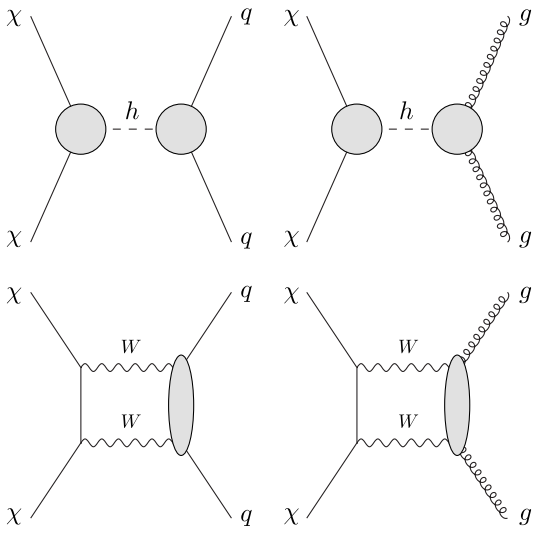

Figure 1. Diagrams for wino-nucleon scattering.

gluon, respectively [71–74]. These diagrams are classified into two types; one is the Higgs exchange type like the upper two diagrams and the other is the box diagrams corresponding to the lower two. We separately discuss each two type.

The Higgs contribution only induces the scalar-type operators. For the NLO-level calculation, we need to evaluate the two- and three-loop diagrams for the quark and gluon scalar-type operators, respectively.

For the box-type contribution, on the other hand, the NLO-level calculation requires us to determine the Wilson coefficients of the operators $m_q\bar{q}q$, $\frac{\alpha_s}{\pi}G^a_{\mu\nu}G^{a\mu\nu}$, and $\mathcal{O}^i_{\mu\nu}$ to $\mathcal{O}(\alpha_s/\pi)$. We first carry out the OPEs of the correlation function of the electroweak currents, as described in refs. [72, 73]. For the scalar operators, the NLO contribution to the OPEs of the correlation functions of vector and axial-vector currents is evaluated in ref. [94] in the degenerate quark mass limit for each generation. The results are directly applicable to the contribution of the first two generations in our calculation since all of the quarks of the generations may be regarded as massless. Concerning the third generation contribution, the mass difference between top and bottom quarks is significant, and thus the mere use of the results in ref. [94] is not justified. Their contribution is, however, found to be small compared with those of the first two generations. In our calculation, we neglect the NLO contribution of the third generation, and take into account the effects as a theoretical uncertainty. The Wilson coefficients of the twist-2 operators are evaluated in ref. [95] to $\mathcal{O}(\alpha_s/\pi)$ in the massless limit. It is again not possible to use the results for the contribution of the third generation, and thus we will drop the contribution and estimate the effects as a theoretical uncertainty. By evaluating the W boson loop diagrams with this correlation function, we then obtain the Wilson coefficients of the operators in eq. (2.2).

As a result, $C^q_{\rm S}$, $C^i_{\rm T_1}$, and $C^i_{\rm T_2}$ are computed at the two-loop level, while $C^G_{\rm S}$ is evaluated at the three-loop level. In table 3, we summarize the number of loops in diagrams relevant to the NLO calculation for each contribution. They complete the NLO matching condition

JHEP06(2015)097

Operators		Higgs		Box	
Parton	Type	LO	NLO	LO	NLO
Quark	Scalar $C_{\rm S}^q$	1-loop	2-loop	-	2-loop
(1st&2nd)	Twist-2 $C_{\rm T_{1,2}}^q$	-	-	1-loop	2-loop
Quark	Scalar $C_{\rm S}^b$	1-loop	2-loop	1-loop	2-loop (neglected)
(b-quark)	Twist-2 $C_{\rm T_{1,2}}^b$	-	-	1-loop	2-loop (neglected)
Gluon	Scalar $C_{\rm S}^G$	2-loop	3-loop	2-loop	3-loop
(1st & 2nd)	Twist-2 $C_{\rm T_{1,2}}^G$	-	-	-	2-loop
Gluon	Scalar $C_{\rm S}^G$	2-loop	3-loop	2-loop	3-loop (3rd gen. neglected)
(3rd)	Twist-2 $C_{\rm T_{1,2}}^G$	-	-	-	2-loop (3rd gen. neglected)

Table 3. Number of loops in diagrams relevant to the $\mathcal{O}(\alpha_s/\pi)$ calculation for each operator. We also show where we neglect the third generation contribution at the NLO. Here "−" means that there is no contribution or the contribution vanishes.

for each Wilson coefficient at the electroweak scale μ_W. In addition, we show in the table where we ignore the third generation contribution. As we will see below, the effect of dropping the NLO third-generation contribution is actually negligible.

2.3.1 Higgs exchange

The Higgs exchange processes are induced by the effective coupling of the wino DM with the Higgs boson. They only give the scalar-type interactions as we show in table 3.

In the case that the wino DM is close to the electroweak eigenstate, the coupling is generated at one-loop level:

$$\mathcal{L}_{\chi\chi h} = -\frac{1}{2} c_{\rm H}(w)\ \bar{\chi}^0 \chi^0 h^0 \,, \tag{2.14}$$

where $w \equiv m_W^2/M^2$ with m_W and M being the masses of W boson and wino, respectively, and $c_{\rm H}(w) = \frac{g_2^3}{(4\pi)^2} g_{\rm H}(w)$. Here $g_{\rm H}(x)$ is a mass function presented in ref. [71].[2] By using the effective coupling we readily obtain the LO matching condition for the scalar-type quark operators as

$$C_{\rm S}^q(\mu_W)|_{\rm LO} = \frac{\alpha_2^2}{4 m_W m_h^2} g_{\rm H}(w) \ . \tag{2.15}$$

Here m_h is the mass of the Higgs boson and $\alpha_2 \equiv g_2^2/(4\pi)$. To evaluate the NLO matching condition, one needs to evaluate the QCD corrections in the full and effective theories at two- and one-loop levels, respectively. These corrections turn out to be equivalent, and thus the matching condition does not differ from the above equation, i.e.,

$$C_{\rm S}^q(\mu_W) = \frac{\alpha_2^2}{4 m_W m_h^2} g_{\rm H}(w) \,, \tag{2.16}$$

to the NLO in perturbation theory.

[2]The mass functions used in text are collected in appendix A.

JHEP06(2015)097

For the scalar-type gluon operator, the one-loop long-distance contribution by the scalar-type quark operators is subtracted from the two-loop contribution in the full theory so that only the top-quark contribution is included in $C_{\rm S}^G$. Then, we have [91]

$$C_{\rm S}^G(\mu_W)|_{\rm LO} = -\frac{\alpha_2^2}{48 m_W m_h^2} g_{\rm H}(w) \,. \tag{2.17}$$

At the NLO, the above expression is modified to [96, 97]

$$C_{\rm S}^G(\mu_W) = -\frac{\alpha_2^2}{48 m_W m_h^2} g_{\rm H}(w) \left[1 + \frac{11}{4\pi}\alpha_s(\mu_W)\right] \,. \tag{2.18}$$

Notice that it contains no logarithmic terms like those containing a factor of $\ln(m_t/\mu_W)$. This is because $\frac{\alpha_s}{\pi} G^a_{\mu\nu} G^{a\mu\nu}$ is renormalization-group invariant up to this order in perturbation theory.

2.3.2 Box type

Let us move on to the contribution of the box diagrams. They induce both scalar-type and twist-2 operators. To compute the effective operators, we first consider the OPEs of the correlation function of the charged currents:

$$\Pi^W_{\mu\nu}(q) \equiv i \int d^4x e^{iq\cdot x}\; T\{J^W_\mu(x) J^W_\nu(0)^\dagger\} \,, \tag{2.19}$$

where

$$J^W_\mu \equiv \sum_{i=1,2,3} \frac{g_2}{\sqrt{2}} \overline{u}_i \gamma_\mu P_L d_i \,, \tag{2.20}$$

with $P_L \equiv (1-\gamma_5)/2$. We evaluate the Wilson coefficients of the scalar and twist-2 operators in the OPEs up to the NLO in α_s/π.

We first consider the scalar part. It is convenient to decompose the correlator into the transverse and the longitudinal parts as

$$\Pi^W_{\mu\nu}(q)|_{\rm scalar} = \left(-g_{\mu\nu} + \frac{q_\mu q_\nu}{q^2}\right)\Pi^W_T(q^2) + \frac{q_\mu q_\nu}{q^2}\Pi^W_L(q^2) \,, \tag{2.21}$$

where

$$\Pi^W_T(q^2) = \sum_q c^q_{W,S}(q^2;\mu_W) m_q \bar{q}q + c^G_{W,S}(q^2;\mu_W)\frac{\alpha_s}{\pi} G^a_{\mu\nu} G^{a\mu\nu} \,. \tag{2.22}$$

Here we give only the transverse part since the longitudinal one does not contribute to $C_{\rm S}^q$ and $C_{\rm S}^G$ [72, 73]. As for the contribution to the scalar-type quark operators of the first two generations, there is no $\mathcal{O}(\alpha_s^0)$ term since the charged current J^W_μ is pure chiral (we take small quark mass limit for $q = u, d, s, c, b$). Thus, only the one-loop diagrams are relevant in this case. It readily follows from the results given in ref. [94], in which the correlation functions for vector and axial currents are evaluated with the OPEs, that

$$c^q_{W,S}(q^2;\mu_W) = -\frac{\alpha_s(\mu_W)}{4\pi}\frac{g_2^2}{q^2} \,, \tag{2.23}$$

for $q = u, d, s, c$. On the other hand, the tree-level contribution of the bottom quark to the scalar-type operator does not vanish because of the large top-quark mass. We have

$$c^b_{W,S}(q^2;\mu_W) = \frac{g_2^2 m_t^2}{8(q^2-m_t^2)^2}\ . \tag{2.24}$$

Here, as mentioned above, we neglect the NLO contribution and take its effects into account as a theoretical uncertainty. The gluon contribution of the first two generations is also obtained straightforwardly from ref. [94]. The contribution of the third generation quarks, however, is not evaluated reliably by means of the method used in ref. [94] due to the large mass of top quark. Here again, we neglect the NLO effects and consider them as a theoretical uncertainty. As a result, we obtain

$$c^G_{W,S}(q^2;\mu_W) = \frac{g_2^2}{48q^2}\left[2\times\left(1+\frac{7}{6}\frac{\alpha_s(\mu_W)}{\pi}\right)+\left(\frac{q^2}{q^2-m_t^2}\right)\right], \tag{2.25}$$

where the first and second terms in bracket correspond to the contribution of the first two generations and the third generation, respectively.

Next, we consider the twist-2 part. For the contribution of $q = u, d, s, c$ to the quark twist-2 operators, the relevant parts are written as

$$\Pi^W_{\mu\nu}(q)|^Q_{(1,2)} = \sum_{q=u,d,s,c}\frac{g_2^2}{2}\left[-\left(\frac{g_{\mu\rho}g_{\nu\sigma}q^2 - g_{\mu\rho}q_\nu q_\sigma - q_\mu q_\rho g_{\nu\sigma} + g_{\mu\nu}q_\rho q_\sigma}{(q^2)^2}\right)c^q_{W,2} + \left(g_{\mu\nu}-\frac{q_\mu q_\nu}{q^2}\right)\frac{q_\rho q_\sigma}{(q^2)^2}c^q_{W,L}\right]\mathcal{O}^{q\rho\sigma}\ . \tag{2.26}$$

The Wilson coefficients $c^q_{W,2}$ and $c^q_{W,L}$ are evaluated in refs. [95] as follows:

$$\begin{aligned} c^q_{W,2}(\mu_W) &= 1+\frac{\alpha_s(\mu_W)}{4\pi}\left[-\frac{1}{2}\left(\frac{64}{9}\right)\ln\left(\frac{-q^2}{\mu_W^2}\right)+\frac{4}{9}\right], \\ c^q_{W,L}(\mu_W) &= \frac{\alpha_s(\mu_W)}{4\pi}\left[\frac{16}{9}\right]. \end{aligned} \tag{2.27}$$

For the third generation contribution, on the other hand, we take into account top mass in the LO part and neglect the NLO part as mentioned above. As a result, we have

$$\Pi^W_{\mu\nu}(q)|^Q_{(3)} = -\frac{g_2^2}{2}\frac{1}{(q^2-m_t^2)^2}\left[(q^2-m_t^2)g_{\mu\rho}g_{\nu\sigma} - g_{\mu\rho}q_\nu q_\sigma - q_\mu q_\rho g_{\nu\sigma} + g_{\mu\nu}q_\rho q_\sigma\right]c^b_{W,3}\mathcal{O}^{b\rho\sigma}\ , \tag{2.28}$$

with

$$c^b_{W,3} = 1+\frac{\alpha_s(\mu_W)}{4\pi}\left[-\frac{1}{2}\left(\frac{64}{9}\right)\ln\left(\frac{-q^2}{\mu_W^2}\right)\right]. \tag{2.29}$$

Note that we have included the logarithmic part though it is induced at the NLO; otherwise, the Wilson coefficient shows wrong dependence on the factorization scale μ_W. Finally let

us derive the gluon twist-2 operator. It is always induced at $\mathcal{O}(\alpha_s/\pi)$. For the contribution of massless quarks, we use the results given in refs. [95]. The result is

$$\Pi^W_{\mu\nu}(q)|^G_{(1,2)} = \frac{g_2^2}{2}\left[-\left(\frac{g_{\mu\rho}g_{\nu\sigma}q^2 - g_{\mu\rho}q_\nu q_\sigma - q_\mu q_\rho g_{\nu\sigma} + g_{\mu\nu}q_\rho q_\sigma}{(q^2)^2}\right)c^G_{W,2} + \left(g_{\mu\nu} - \frac{q_\mu q_\nu}{q^2}\right)\frac{q_\rho q_\sigma}{(q^2)^2}c^G_{W,L}\right]\mathcal{O}^{G\rho\sigma}\,, \tag{2.30}$$

where

$$c^G_{W,2}(\mu_W) = 4\times\frac{\alpha_s(\mu_W)}{4\pi}\left[-\frac{1}{2}\left(\frac{4}{3}\right)\ln\left(\frac{-q^2}{\mu_W^2}\right)+\frac{1}{2}\right],$$
$$c^G_{W,L}(\mu_W) = 4\times\frac{\alpha_s(\mu_W)}{4\pi}\left[-\frac{2}{3}\right], \tag{2.31}$$

with a factor of four counting the number of the first two generation quarks. As before, we neglect the NLO contribution of the third generation quarks but keep its logarithmic part in order to guarantee the appropriate scale dependence. This reads

$$\Pi^W_{\mu\nu}(q)|^G_{(3)} = -\frac{g_2^2}{2}\frac{1}{(q^2-m_t^2)^2}\left[(q^2-m_t^2)g_{\mu\rho}g_{\nu\sigma} - g_{\mu\rho}q_\nu q_\sigma - q_\mu q_\rho g_{\nu\sigma} + g_{\mu\nu}q_\rho q_\sigma\right] \times c^G_{W,3}\mathcal{O}^{G\rho\sigma}\,, \tag{2.32}$$

with

$$c^G_{W,3} = \frac{\alpha_s(\mu_W)}{4\pi}\left[-\frac{1}{2}\left(\frac{4}{3}\right)\ln\left(\frac{-q^2}{\mu_W^2}\right)\right]. \tag{2.33}$$

Then, the sum of the above contributions gives the total twist-2 contribution:

$$\Pi^W_{\mu\nu}(q)|_{\rm twist2} = \Pi^W_{\mu\nu}(q)|^Q_{(1,2)} + \Pi^W_{\mu\nu}(q)|^Q_{(3)} + \Pi^W_{\mu\nu}(q)|^G_{(1,2)} + \Pi^W_{\mu\nu}(q)|^G_{(3)}\,. \tag{2.34}$$

Our remaining task is to obtain the Wilson coefficients of the effective operators in eq. (2.2) by computing another loop with the electroweak current correlator $\Pi^W_{\mu\nu}(q)$. For the scalar-type operators, we have

$$C^q_{\rm S}(\mu_W) = \frac{\alpha_2^2}{m_W^3}\frac{\alpha_s(\mu_W)}{4\pi}[-12 g_{\rm B1}(w)]\,, \qquad (\text{for } \ q=u,d,s,c)\,,$$
$$C^b_{\rm S}(\mu_W) = \frac{\alpha_2^2}{m_W^3}\left[(-3)g_{\rm btm}(w,\tau)\right],$$
$$C^G_{\rm S}(\mu_W) = \frac{\alpha_2^2}{4m_W^3}\left[\left(2+\frac{7}{3}\frac{\alpha_s(\mu_W)}{\pi}\right)g_{\rm B1}(w) + g_{\rm top}(w,\tau)\right], \tag{2.35}$$

where $\tau \equiv m_t^2/M^2$. The mass function $g_{\rm B1}(x)$ is given in ref. [71], and $g_{\rm top}(x,y)$ and $g_{\rm btm}(x,y)$ are equivalent to $g^{(1)}_{\rm B3}(x,y)$ and $g^{(2)}_{\rm B3}(x,y)$ in ref. [73], respectively. These functions are also presented in appendix A.

JHEP06(2015)097

For the twist-2 type operators, on the other hand, we have

$$
\begin{aligned}
C^q_{\mathrm{T}_i}(\mu_W) =& \frac{\alpha_2^2}{m_W^3}\left[g_{\mathrm{T}_i}(w,0) + \frac{\alpha_s(\mu_W)}{4\pi}\left(-\frac{32}{9}g^{\log}_{\mathrm{T}_i}(w,0;\mu_W) + \frac{9}{4}g_{\mathrm{T}_i}(w,0) + \frac{16}{9}h_{\mathrm{T}_i}(w)\right)\right], \\
C^b_{\mathrm{T}_i}(\mu_W) =& \frac{\alpha_2^2}{m_W^3}\left[g_{\mathrm{T}_i}(w,\tau) + \frac{\alpha_s(\mu_W)}{4\pi}\left(-\frac{32}{9}g^{\log}_{\mathrm{T}_i}(w,\tau;\mu_W)\right)\right], \\
C^G_{\mathrm{T}_i}(\mu_W) =& \frac{\alpha_2^2}{m_W^3}\frac{\alpha_s(\mu_W)}{4\pi}\times \\
& \left[4\times\left(-\frac{2}{3}g^{\log}_{\mathrm{T}_i}(w,0;\mu_W) + \frac{1}{2}g_{\mathrm{T}_i}(w,0) - \frac{2}{3}h_{\mathrm{T}_i}(w)\right) - \frac{2}{3}g^{\log}_{\mathrm{T}_i}(w,\tau;\mu_W)\right],
\end{aligned}
\tag{2.36}
$$

where the functions $g_{\mathrm{T}_i}(x,y)$, $h_{\mathrm{T}_i}(x)$ and $g^{\log}_{\mathrm{T}_i}(x,y;\mu_W)$ are given in appendix A. $g_{\mathrm{T}_i}(x,0)$ agrees with $g_{\mathrm{T}_i}(x)$ in, e.g., ref. [71]. The terms proportional to $g^{\log}_{\mathrm{T}_i}(x,y)$ come from the logarithmic terms in the OPEs of the correlation function of the charged currents, while the terms with $g_{\mathrm{T}_i}(x,y)$ and $h_{\mathrm{T}_i}(x)$ are from the non-logarithmic terms in $c^{q/b/G}_{W,2}$ and $c^{q/G}_{W,L}$, respectively. The NLO contribution to the gluon twist-2 operator is also given in refs. [79, 82]. Here we note that to obtain the proper dependence of the above coefficients on the scale μ_W, we need to include all of the NLO corrections. Otherwise, the mismatch in the scale dependence between the matching conditions and the RGEs causes large uncertainties.

To that end, it is important to appropriately perform the order counting with respect to α_s/π. Especially, the two-loop contribution to $C^G_{\mathrm{T}_i}$ should be regarded as the NLO in α_s/π,[3] not the LO, which is contrary to the case of the gluon scalar operator C^G_{S}; in this case, the two-loop contribution is the LO in α_s/π. Our convention for the definition of the gluon operators clarifies this order counting.

As we have already commented several times, we neglect the NLO contribution of the third generation quarks. Indeed, we expect that its significance is quite small, and thus we safely regard it as a theoretical uncertainty. In figure 2 we compare the mass functions corresponding to the LO third generation contributions with those of the LO massless quark contributions, which corresponds to $g_{\mathrm{top}}(w,\tau)/g_{\mathrm{B1}}(w)$, $g_{\mathrm{T}_1}(w,\tau)/g_{\mathrm{T}_1}(w,0)$, and $g_{\mathrm{T}_2}(w,\tau)/g_{\mathrm{T}_2}(w,0)$. $g_{\mathrm{btm}}(w,\tau)/g_{\mathrm{B1}}(w)$ is also shown as its contribution to C^G_{S} via integration of the bottom quark is given by $-C^b_{\mathrm{S}}/12$. It is found that the LO third generation contributions are smaller than those of the first and second generations by almost an order of magnitude. Hence, we expect that the NLO contributions of the third generation are also considerably small compared with those of the other two generations. This allows us to ignore the third-generation NLO contribution, and treat it as a theoretical uncertainty.

2.4 Renormalization group equations and matching conditions

The effective operators are scale dependent and their scale evolution is described by the RGEs. During the RG evolution, heavy quarks are integrated out around their mass scale.

[3] One may easily check that the logarithmic parts in the NLO contribution to the twist-2 operators reproduce the one-loop RGEs presented in section 2.4. This justifies the order counting discussed here.

JHEP06(2015)097

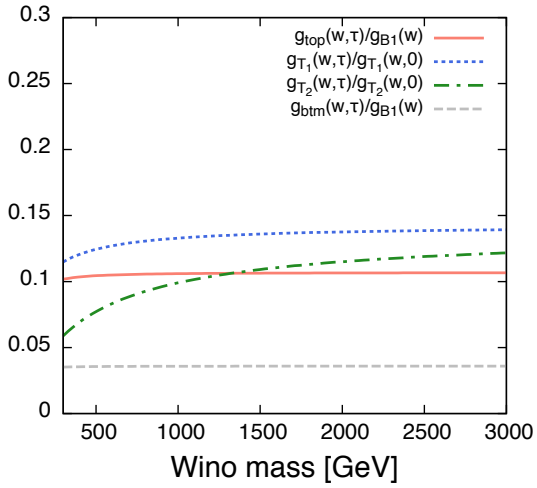

Figure 2. Comparison of $g_{\rm top}(w,\tau)$, $g_{\rm T_1}(w,\tau)$, $g_{\rm T_2}(w,\tau)$, and $g_{\rm btm}(w,\tau)$ with $g_{\rm B1}(w)$, $g_{\rm T_1}(w,0)$, $g_{\rm T_2}(w,0)$, and $g_{\rm B1}(w)$ in red solid, blue dotted, green dash-dotted, and gray dashed lines, respectively, to show smallness of third generation contributions.

Thus we need to match the theories above and below the threshold. Here we summarize the RGEs and the matching conditions.

To begin with, we write down beta-function of α_s and anomalous dimension of quark mass operator:

$$\beta(\alpha_s) = (2b_1)\frac{\alpha_s^2}{4\pi} + (2b_2)\frac{\alpha_s^3}{(4\pi)^2}\,, \tag{2.37}$$

$$\gamma_m = -6C_F\frac{\alpha_s}{4\pi}\,, \tag{2.38}$$

with $b_1 = -\frac{11}{3}N_c + \frac{2}{3}N_f$, $b_2 = -\frac{34}{3}N_c^2 + \frac{10}{3}N_cN_f + 2C_FN_f$. ($N_c = 3$ is the number of colors, N_f denotes the number of quark flavors in an effective theory and C_F is the quadratic Casimir invariant defined by $C_F \equiv \frac{N_c^2-1}{2N_c}$.) Here for the $\overline{\rm MS}$ quark masses, we use the one-loop anomalous dimension since their effects first appear at the NLO level as we will see below soon.

Now we give the RGEs for the Wilson coefficients of the above operators. First, we consider the RGEs for the scalar-type operators. To that end, notice that the quark mass operator is RG invariant in a mass-independent renormalization scheme like the $\overline{\rm MS}$ scheme, i.e.,

$$\mu\frac{d}{d\mu}m_q\bar{q}q = 0\ . \tag{2.39}$$

To evaluate the evolution of the gluon scalar operator, we use the trace anomaly formula (2.5). Differentiating eq. (2.5), we then obtain the differential equation for the gluonic

JHEP06(2015)097

scalar operator $\frac{\alpha_s}{\pi}G^a_{\mu\nu}G^{a\mu\nu}$. As a result, we have[4]

$$\mu\frac{d}{d\mu}(C^q_{\rm S}, C^G_{\rm S}) = (C^q_{\rm S}, C^G_{\rm S})\ \Gamma_{\rm S}\,, \tag{2.40}$$

where $\Gamma_{\rm S}$ is a $(N_f+1)\times(N_f+1)$ matrix given by

$$\Gamma_{\rm S} = \begin{pmatrix} 0 & \cdots & 0 & 0 \\ \vdots & \ddots & \vdots & \vdots \\ 0 & \cdots & 0 & 0 \\ -4\alpha_s^2\frac{d\gamma_m}{d\alpha_s} & \cdots & -4\alpha_s^2\frac{d\gamma_m}{d\alpha_s} & \alpha_s^2\frac{d}{d\alpha_s}\left(\frac{\beta(\alpha_s)}{\alpha_s^2}\right) \end{pmatrix}, \tag{2.41}$$

The solutions of the RGEs are given as follows:

$$C^q_{\rm S}(\mu) = C^q_{\rm S}(\mu_0) - 4C^G_{\rm S}(\mu_0)\frac{\alpha_s^2(\mu_0)}{\beta(\alpha_s(\mu_0))}(\gamma_m(\mu)-\gamma_m(\mu_0))\,, \tag{2.42}$$

$$C^G_{\rm S}(\mu) = \frac{\beta(\alpha_s(\mu))}{\alpha_s^2(\mu)}\frac{\alpha_s^2(\mu_0)}{\beta(\alpha_s(\mu_0))}C^G_{\rm S}(\mu_0)\ . \tag{2.43}$$

Eq. (2.42) shows that the anomalous dimension at $\mathcal{O}(\alpha_s)$, i.e. eq. (2.38), is enough for the NLO calculation.

Next, we consider the RGEs for the twist-2 operators. The two-loop anomalous dimension matrix of the operators is evaluated as [99, 100]

$$\mu\frac{d}{d\mu}(C^q_{{\rm T}_i}, C^G_{{\rm T}_i}) = (C^q_{{\rm T}_i}, C^G_{{\rm T}_i})\ \Gamma_{\rm T}\,, \tag{2.44}$$

with $\Gamma_{\rm T}$ a $(N_f+1)\times(N_f+1)$ matrix:

$$\Gamma_{\rm T} = \begin{pmatrix} \gamma_{qq} & 0 & \cdots & 0 & \gamma_{qg} \\ 0 & \gamma_{qq} & & \vdots & \vdots \\ \vdots & & \ddots & 0 & \vdots \\ 0 & \cdots & 0 & \gamma_{qq} & \gamma_{qg} \\ \gamma_{gq} & \cdots & \cdots & \gamma_{gq} & \gamma_{gg} \end{pmatrix}, \tag{2.45}$$

where

$$\begin{aligned}
\gamma_{qq} &= \frac{16}{3}C_F\cdot\frac{\alpha_s}{4\pi} + \left(-\frac{208}{27}C_FN_f - \frac{224}{27}C_F^2 + \frac{752}{27}C_FN_c\right)\left(\frac{\alpha_s}{4\pi}\right)^2, \\
\gamma_{qg} &= \frac{4}{3}\cdot\frac{\alpha_s}{4\pi} + \left(\frac{148}{27}C_F + \frac{70}{27}N_c\right)\left(\frac{\alpha_s}{4\pi}\right)^2, \\
\gamma_{gq} &= \frac{16}{3}C_F\cdot\frac{\alpha_s}{4\pi} + \left(-\frac{208}{27}C_FN_f - \frac{224}{27}C_F^2 + \frac{752}{27}C_FN_c\right)\left(\frac{\alpha_s}{4\pi}\right)^2, \\
\gamma_{gg} &= \frac{4}{3}N_f\cdot\frac{\alpha_s}{4\pi} + \left(\frac{148}{27}C_FN_f + \frac{70}{27}N_cN_f\right)\left(\frac{\alpha_s}{4\pi}\right)^2.
\end{aligned} \tag{2.46}$$

[4] In fact, we implicitly assume that the operators are to be evaluated between the on-shell states. As discussed in refs. [96, 98], during the RG flow, the scalar operators mix with other (gauge-variant) operators whose on-shell matrix elements vanish.

JHEP06(2015)097

Finally we give the threshold corrections at the scale where heavy quarks are integrated out. For example, in the vicinity of the bottom-quark threshold $\mu_b \simeq m_b$, we match the strong gauge coupling constant and the Wilson coefficients as

$$\frac{1}{\alpha_s(\mu_b)|_{N_f=4}} = \frac{1}{\alpha_s(\mu_b)|_{N_f=5}} + \frac{1}{3\pi}\ln\left(\frac{\mu_b}{m_b}\right), \tag{2.47}$$

and

$$\begin{aligned}
C_{\rm S}^q(\mu_b)|_{N_f=4} =& C_{\rm S}^q(\mu_b)|_{N_f=5}\,, \\
[\alpha_s C_{\rm S}^G](\mu_b)|_{N_f=4} =& -\frac{\alpha_s(\mu_b)}{12}\left[1+\frac{\alpha_s(\mu_b)}{4\pi}\left(11+\frac{2}{3}\ln\frac{m_b^2}{\mu_b^2}\right)\right] C_{\rm S}^b(\mu_b)|_{N_f=5} \\
&+\left[1+\frac{\alpha_s(\mu_b)}{4\pi}\frac{2}{3}\ln\frac{m_b^2}{\mu_b^2}\right][\alpha_s C_{\rm S}^G](\mu_b)|_{N_f=5}\,, \\
C_{{\rm T}_i}^q(\mu_b)|_{N_f=4} =& C_{{\rm T}_i}^q(\mu_b)|_{N_f=5}\,, \\
C_{{\rm T}_i}^G(\mu_b)|_{N_f=4} =& \left[1+\frac{\alpha_s(\mu_b)}{4\pi}\frac{2}{3}\ln\frac{m_b^2}{\mu_b^2}\right] C_{{\rm T}_i}^G(\mu_b)|_{N_f=5} + \frac{\alpha_s(\mu_b)}{4\pi}\frac{2}{3}\ln\frac{m_b^2}{\mu_b^2} C_{{\rm T}_i}^b(\mu_b)|_{N_f=5}\,,
\end{aligned} \tag{2.48}$$

with $q = u, d, s, c$ for the first and third equations.[5] In the following section, we estimate the uncertainties coming from the neglect of the higher order perturbation by varying the matching scale μ_b around the $\mu_b \simeq m_b$. We repeat a similar procedure for the charm-quark threshold around $\mu_c \simeq m_c$.

Here we note that besides the above threshold corrections, the higher dimension operators suppressed by a power of the threshold quark mass are also generated in general. For instance, if the scalar-type quark operator is integrated out at a quark threshold m_Q, then we will obtain the following dimension-nine operators at one-loop level [98, 101]:

$$-\left[\frac{\alpha_s(m_Q)}{60\pi m_Q^2}(D^\nu G^a_{\nu\mu})(D^\rho G^a_{\rho\mu})\bar{\chi}^0\chi^0 + \frac{g_s\alpha_s(m_Q)}{720\pi m_Q^2} f_{abc} G^a_{\mu\nu} G^{b\mu\rho} G^c_{\nu\rho}\bar{\chi}^0\chi^0\right] C_{\rm S}^Q(m_Q)\,, \tag{2.49}$$

where f_{abc} is the SU(3) structure constant. In particular, those generated at the charm-quark threshold give the largest effects. By using the naive dimensional analysis, we see that their contribution to the nucleon matrix element may give a correction by a factor of $\Lambda_{\rm QCD}^2/m_c^2 = \mathcal{O}(0.1)$, which could be additionally suppressed by the prefactors of these operators. Since we do not know precise values of the nucleon matrix elements of the operators in eq. (2.49), we should also consider their effects as an uncertainty.

3 Results

Now we compute the wino-nucleon scattering cross section and evaluate the theoretical uncertainties. We first separately consider the scalar and twist-2 contributions to the wino-nucleon effective coupling in section 3.1 and 3.2, respectively. Then, we show the

[5] The matching condition for $C_{{\rm T}_i}^G$ here differs from that given in refs. [79, 82].

JHEP06(2015)097

Strong coupling constant $\alpha_s(m_Z)$ [102]	0.1185 ± 0.0006
Higgs pole mass m_h [103, 104]	$125.03 \pm 0.27\,\mathrm{GeV}$
Top-quark pole mass m_t [105]	$173.34 \pm 0.76\,\mathrm{GeV}$

Table 4. Input parameters.

result for the scattering cross section in the following subsection. In table 4, we summarize the input parameters we use in our computation. For the mass of top quark, we use the pole mass as an input parameter, and convert it to the $\overline{\mathrm{MS}}$ mass using the one-loop relation:

$$m_t = \overline{m}_t(\overline{m}_t)\left[1 + \frac{4\alpha_s(\overline{m}_t)}{3\pi}\right], \tag{3.1}$$

where $\overline{m}_t$ denotes the $\overline{\mathrm{MS}}$ top mass. In what follows, we only use the $\overline{\mathrm{MS}}$ mass so we drop the bar for brevity.

3.1 Scalar part

The spin-independent effective coupling of the wino with nucleon is defined by

$$\mathcal{L}_{\mathrm{SI}}^{(N)} = f^N \bar{\chi}^0 \chi^0 \overline{N} N \ . \tag{3.2}$$

The contribution of the scalar operators to the coupling is given by

$$f_{\mathrm{scalar}}^N = \sum_{q=u,d,s} C_{\mathrm{S}}^q(\mu_{\mathrm{had}}) \langle N | m_q \bar{q} q | N \rangle + C_{\mathrm{S}}^G(\mu_{\mathrm{had}}) \langle N | \frac{\alpha_s}{\pi} G_{\mu\nu}^a G^{a\mu\nu} | N \rangle \,, \tag{3.3}$$

where we take the hadron scale $\mu_{\mathrm{had}} = 1\,\mathrm{GeV}$ with $N_f = 3$ active quarks. Figure 3 shows f_{scalar}^p with various types of errors.

In figure 3 (a) f_{scalar}^p at the LO (blue dashed) and NLO (red solid) with corresponding bands showing the theoretical error due to the perturbative calculation are shown. In the plot the uncertainty coming from lack of the NLO contribution of the third generation, which is multiplied by a factor of five just for the purpose of presentation, is also shown (gray band). For the evaluation of the error from the ignorance of higher order contribution in perturbation, we vary each matching scale by a factor of two; i.e., $m_c/2 \leq \mu_c \leq 2m_c$, $m_b/2 \leq \mu_b \leq 2m_b$, $m_Z/2 \leq \mu_W \leq 2m_Z$. The prescription is, however, less effective for the scalar-type operators since these operators are almost scale-invariant. For this reason, when evaluating the error resulting from the quark threshold matching for the NLO (LO) calculation, we use the NNLO (NLO) matching conditions to artificially generate the logarithmic dependence of the Wilson coefficients on the scale by using the mismatch between the matching conditions and RGEs. The NLO matching conditions are given in eq. (2.48), while the NNLO ones are found in ref. [106]. In addition, for the LO contribution, we evaluate the uncertainty caused by the electroweak-scale matching by merely multiplying the LO contribution by a factor of α_s/π. Since the scalar-type operators are scale-invariant at the LO, it is impossible to estimate the LO uncertainty from the electroweak-scale matching by varying the scale μ_W. At the NLO, on the other hand, we are able to estimate the

JHEP06(2015)097

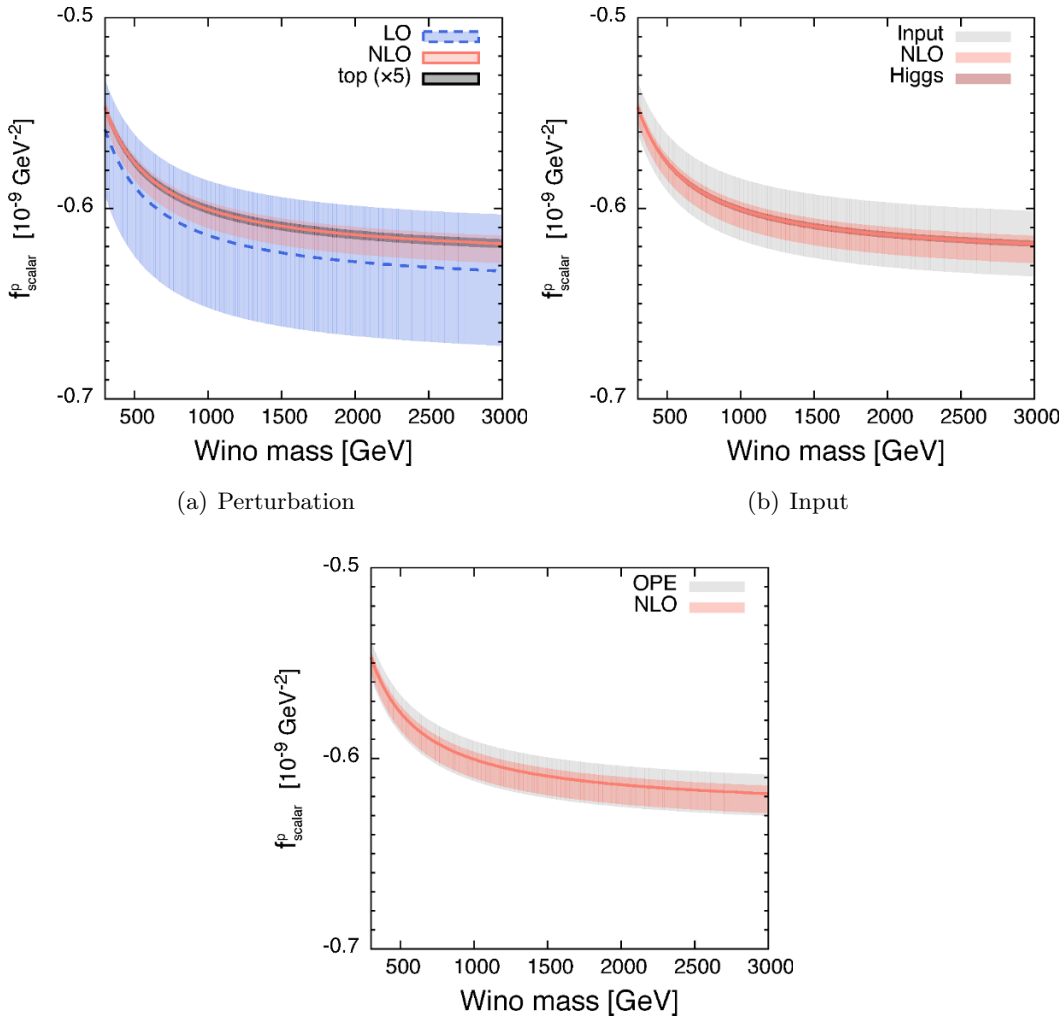

(a) Perturbation

(b) Input

(c) OPE

Figure 3. Contribution of scalar-type operators to wino-proton coupling f^p_{scalar}. (a) LO (blue dashed) and NLO (red solid) results with corresponding bands showing uncertainty due to perturbative calculation. Gray band indicates uncertainty coming from lack of NLO contribution of third generation, multiplied by a factor of five. (b) Errors from input parameters (gray), the Higgs mass (dark red), compared with NLO error (pink). (c) Uncertainty from truncating higher dimension operators at each quark threshold (gray band), compared with NLO perturbative QCD uncertainty (pink band).

uncertainty with the scale variation since the NLO RGEs yield the scale dependence of the scalar operators.

The error from the LO perturbative calculation is more than 5%, which reduces to a few % level with the NLO calculation. The upper errors are smaller than the lower errors in the LO and NLO perturbative calculations in the figure 3 (a). This comes from difference between $\alpha_s(m_Q/2)$ and $\alpha_s(2m_Q)$ for $Q = b, c$. On the other hand, as for the uncertainty due

JHEP06(2015)097

to the lack of the third-generation NLO contribution, we estimate its effect by multiplying the LO contribution by a factor of α_s/π. From the figure, we find that the ignorance of the third-generation NLO contribution only gives a negligible effect on the resultant value. The effect is much smaller than the uncertainty due to the perturbative calculation.

Figure 3 (b) shows comparison of the uncertainty in the NLO perturbative QCD calculation (pink) with that from the errors in the input parameters we have used in the calculation (gray). Among them, the uncertainty coming from the Higgs mass error is especially shown in the dark red band. We see that thanks to the NLO calculation the perturbative error now becomes smaller than the error from the input parameters, though they are still of the same order of the magnitude.

Finally we plot the theoretical uncertainty which could arise due to the higher dimension operators induced at each quark threshold in figure 3 (c). To evaluate the effects of the higher dimension operators, we vary the scalar gluon contribution induced at the charm-quark threshold by 2%, which is expected from the naive dimensional analysis as discussed in section 2.4.[6] Since the higher dimension operators generated at the bottom-quark threshold are suppressed by the bottom quark mass, their effects are negligible. As seen from the figure, this uncertainty may be as large as the NLO perturbative QCD error. To reduce the uncertainty, one of the most efficient ways is to use the nucleon matrix elements computed above the charm-quark threshold, say, at the scale of 2 GeV. In this case, we need to evaluate the charm-quark content in nucleon, $f_{T_c}^{(N)} = \langle N|m_c\bar{c}c|N\rangle/m_N$, as well. Currently, the QCD lattice simulations are not able to compute it accurately [107]. If this quantity is evaluated with good precision in the future, then the uncertainty due to the higher dimension operators will be significantly reduced. We expect that the perturbative QCD error will also decrease, since we do not need the charm-quark threshold matching procedure any more. Thus, we strongly encourage the development in this field.

3.2 Twist-2 part

Contrary to the scalar-type operators, the twist-2 operators have the scale dependence at the leading order in α_s. Therefore, it is necessary to determine the appropriate scale for the matching of the full theory onto the effective theory in order not to suffer from large logarithmic factors. To that end, we require that the logarithmic dependent parts $g_{\mathrm{T}_i}^{\log}$ in the Wilson coefficients presented in eq. (2.36) should not be large, say, within $\mathcal{O}(1)$. Since the terms proportional to $g_{\mathrm{T}_i}^{\log}$ come from the logarithmic terms in the OPEs of the correlation function of the charged currents, this condition guarantees the validity of the perturbative QCD expansion. In figure 4, we show $g_{\mathrm{T}_i}^{\log}(w, 0; \mu_W)$ $(i = 1, 2)$ as function of the factorization scale μ_W. Here $M = 3\,\mathrm{TeV}$ (solid) and 300 GeV (dashed). The vertical gray line shows $\mu_W = m_Z$. It turns out that the size of these functions is within $\mathcal{O}(1)$ if one takes the scale μ_W to be around the electroweak scale. This consequence rarely depends on the DM mass. The absolute values for these functions are minimum at a scale

[6] Since the first (second) operator in eq. (2.49) receives additional suppression by a factor of five (sixty) compared with the contribution of the scalar gluon operator, $-\alpha_s/(12\pi)GG\bar{\chi}^0\chi^0$, we estimate the significance of the former contribution as $\sim 2\%$ of that of the scalar-type gluon operator, while the latter contribution is negligible.

JHEP06(2015)097

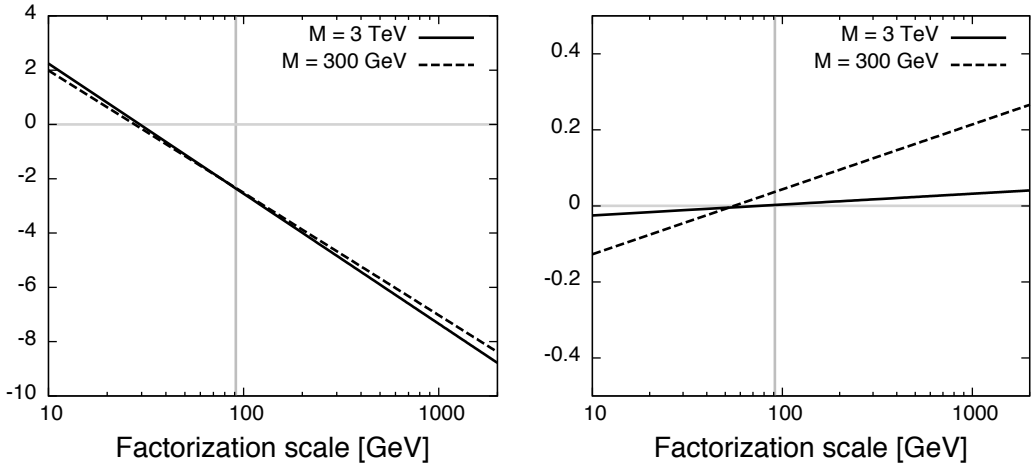

(a) $g^{\log}_{\mathrm{T}_1}(w, 0; \mu_W)$ (b) $g^{\log}_{\mathrm{T}_2}(w, 0; \mu_W)$

Figure 4. $g^{\log}_{\mathrm{T}_i}(w, 0; \mu_W)$ $(i = 1, 2)$ as function of factorization scale μ_W. $M = 3\,\mathrm{TeV}$ (solid) and $300\,\mathrm{GeV}$ (dashed). Vertical gray line shows $\mu_W = m_Z$.

of $\mathcal{O}(10)\,\mathrm{GeV}$, which is much smaller than the DM mass. This observation reflects the fact that the typical scale of the loop momentum flowing in the loop diagrams in figure 1 is around the electroweak scale, as pointed out in ref. [70]. In the following calculation, we take $\mu_W = m_Z$, which assures that $g^{\log}_{\mathrm{T}_i}$ is within $\mathcal{O}(1)$ and thus the perturbative expansion is justified.

To calculate the contribution of the twist-2 operators, we also need to choose the scale at which the nucleon matrix elements of the twist-2 operators are evaluated. As mentioned above, contrary to the case of the scalar-type operators, the twist-2 matrix elements are obtained at various scales. Since the result does not depend on the choice of the scale within the uncertainty of the calculation, it is desirable to choose the scale so that the error in calculation is reduced. Thus, we take it to be the same as the factorization scale, i.e., $\mu = m_Z$. This choice allows us to decrease the error which would arise from the process where the operators are evolved down to the low-energy region; for instance, if one evaluates the matrix elements at a scale $\mu < m_b$, the result suffers from the uncertainty resulting from the bottom-quark mass threshold. See ref. [88] for further discussion.

Now we evaluate the contribution of the twist-2 operators to the SI effective coupling in eq. (3.2), which is given by

$$\begin{aligned}\frac{f^N_{\mathrm{twist2}}}{m_N} =& \frac{3}{4}\sum_q \sum_{i=1,2} C^q_{\mathrm{T}_i}(m_Z)[q^{(N)}(2; m_Z) + \bar{q}^{(N)}(2; m_Z)] \\ & - \frac{3}{4}\sum_{i=1,2} C^G_{\mathrm{T}_i}(m_Z) g^{(N)}(2; m_Z)\,, \end{aligned} \tag{3.4}$$

where q runs over the active quarks ($q = u, d, s, c, b$ for our choice of the scale $\mu = m_Z$).

JHEP06(2015)097

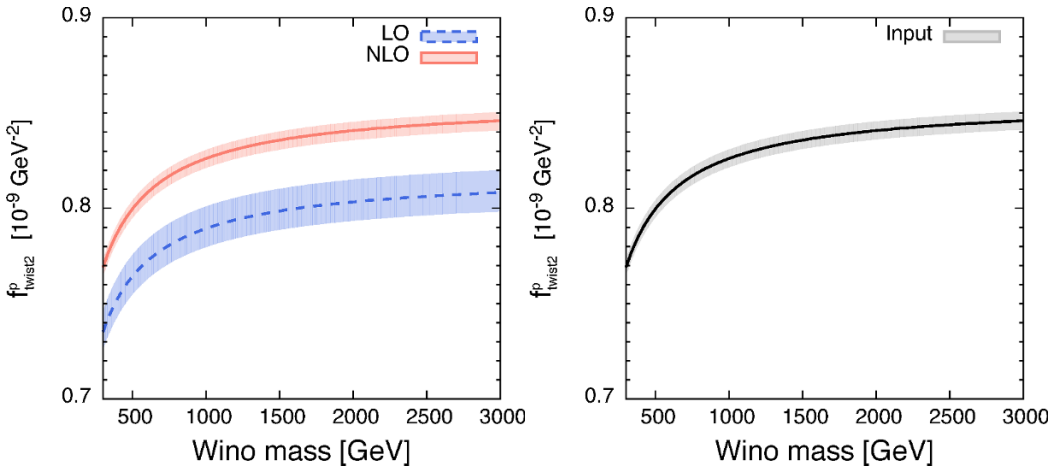

(a) Perturbation (b) Input

Figure 5. Contribution of twist-2 operators to wino-proton coupling $f^p_{\rm twist2}$. (a) LO (blue dashed) and NLO (red solid) results with corresponding bands showing uncertainty due to perturbative calculation. (b) Uncertainty resulting from input error.

In figure 5, we show $f^p_{\rm twist2}$ as function of the wino mass. We compare the LO and NLO results in the left panel, shown in the blue dashed and red solid lines, respectively, with the corresponding bands representing the uncertainties. The uncertainties are evaluated by varying the scale μ_W between $m_Z/2$ and $2m_Z$. Besides, it is found that to drop the NLO contribution of the third generation quarks causes only the negligible effects, so we do not show the error due to the contribution. The $\mathcal{O}(1)\%$ error in the LO computation now reduces to $\sim 0.5\%$ when going to the NLO level, though the central value shifts more than expected, *i.e.* about 5% change. This is due to a large NLO term in $C^q_{{\rm T}_i}$ of eq. (2.36). In the large DM mass limit, the contributions of quarks and gluon at the NLO are 0.90 and -0.047 in $10^{-9}\,{\rm GeV}^{-2}$ unit, respectively, while the quark contribution at the LO is 0.82 in $10^{-9}\,{\rm GeV}^{-2}$ unit.[7] In the right panel of figure 5, we also illustrate the uncertainty resulting from the input error, which turns out to be as large as the NLO uncertainty. The uncertainty mainly comes from those of the PDFs, which we estimate following the method given in ref. [92] with the χ^2 tolerance T taken to be $T = 10$. After all, in the case of the twist-2 contribution, both the NLO and input uncertainties are less than 1%, and thus well controlled compared to the scalar contribution.

3.3 Scattering cross section

Finally, we evaluate the wino-nucleon SI scattering cross section, which is given by

$$\sigma^N_{\rm SI} = \frac{4}{\pi}\left(\frac{M m_N}{M+m_N}\right)^2 |f^N_{\rm scalar} + f^N_{\rm twist2}|^2 \ . \tag{3.5}$$

[7] To be concrete, in $C^q_{{\rm T}_i}$ the NLO term summed over $i = 1, 2$ gives $(\alpha_2^2\alpha_s/4\pi m_W^3) \times (41\pi/12)$ in the large DM mass limit. Here logarithmic term $g^{\rm log}_{{\rm T}_i}$ is neglected for simplicity. See also eqs. (A.18)–(A.31) for the mass functions in the large DM mass limit.

JHEP06(2015)097

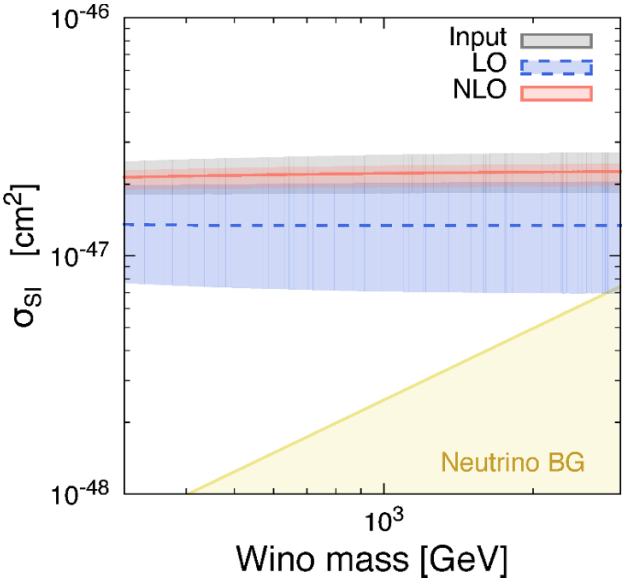

Figure 6. Wino-proton SI scattering cross section. Blue dashed and red solid lines represent LO and NLO results, respectively, with corresponding bands show perturbative uncertainties. Gray band shows uncertainty resulting from the input error. Yellow shaded area corresponds to the region in which neutrino background overcomes DM signal [83].

We plot $\sigma^p_{\rm SI}$ as function of the wino mass in figure 6. Additionally we indicate the parameter region where the neutrino background dominates the the DM-nucleon scattering [83] and then it becomes hard to detect the DM signal in the DM direct detection experiments (yellow shaded). Here we estimate each error by varying the scalar and twist-2 contributions within their uncertainties evaluated above. The result shows that the large uncertainty in the LO computation is significantly reduced once the NLO QCD corrections are included, which is now smaller than that from the input error. In the large DM mass limit, the SI scattering cross section converges to a constant value,

$$\sigma^p_{\rm SI} = 2.3\ ^{+0.2}_{-0.3}\ ^{+0.5}_{-0.4} \times 10^{-47}\ {\rm cm}^2\,, \tag{3.6}$$

where the first and second terms represent the perturbative and input uncertainties, respectively. As seen from figure 6, $\sigma^p_{\rm SI}$ has little dependence on the DM mass; its variation is actually within the uncertainties of the calculation, for the wino mass larger than 270 GeV. Both the scalar and twist-2 contributions depend on the DM mass when the mass is smaller than ~ 1 TeV as shown in figures 3 and 5. However, the dependence in the cross section is accidentally canceled. The NLO result is found to be larger than the LO result by almost 70%. This large enhancement is due to the significant cancellation in the scattering amplitude; because of the cancellation, even an $\mathcal{O}(10)$% correction in each contribution would change the total amplitude significantly. After all, the resultant scattering cross section is well above that of the neutrino background [83], and therefore the future direct detection experiments are promising to test the wino DM scenario.

JHEP06(2015)097

Before concluding the section, we briefly discuss the effects of wino-higgsino mixing. So far, we have assumed that the higgsino mass is heavy enough so that the lightest neutralino is regarded as a pure wino. If the higgsino mass is rather light, however, the wino-higgsino mixing becomes sizable, which allows the lightest neutralino to interact with quarks (gluon) via the tree-level (one-loop) Higgs exchange process. This interaction gives rise to the scalar-type quark operators as

$$C_{\rm S}^{q}|_{\rm tree} \simeq -\frac{g_2^2}{4m_h^2\mu^2}(M + \mu \sin 2\beta)\,, \tag{3.7}$$

where μ is the higgsino mass parameter and $\tan\beta$ is the ratio of the Higgs vacuum expectation values. We assume $|\mu| \gg M$ in the above expression. As shown in ref. [74], this contribution gives a sizable effect if $|\mu| \lesssim \mathcal{O}(10)\,\text{TeV}$. A similar procedure to that given in section 2.3.1 enables us to include this quark contribution as well as the corresponding gluon contribution at the NLO level. In addition, a sizable wino-higgsino mixing modifies the electroweak loop contribution, where W, Z, Higgs and Nambu-Goldstone bosons run in the loop. The effects are evaluated in ref. [81].

4 Electroweakly-interacting DM

Although we have focused on the wino DM in this paper, a similar formalism may be constructed for a more general class of the DM candidates; i.e., an $\text{SU}(2)_L$ multiplet with hypercharge Y that contains a neutral component for DM, and their thermal relic may explain the observed DM density with $\mathcal{O}(1)\,\text{TeV}$ masses. For previous works on such DM candidates, see refs. [108–120]. Some theories beyond the Standard Model actually predict this kind of DM. For example, the higgsino and wino in the SUSY models are representative of the $\text{SU}(2)_L$ multiplet DM. Moreover, such a particle may show up in grand unified theories [121–125], whose stability is explained by a remnant discrete symmetry of extra U(1) symmetries in the theories [126–131].

Before concluding our discussion, we give the results of the NLO calculation for this class of DM candidates. If the DM particle is a fermion, its interactions with quarks and gluon are completely determined by the electroweak gauge interactions,[8] so we consider the fermionic DM candidates in the following discussion. If $Y \neq 0$, the DM is a Dirac fermion, while a Majorana fermion if $Y = 0$. Pure Dirac fermion DM is, however, severely constrained by the direct detection experiments already, since the vector interactions via the Z boson exchange yield too large scattering cross section with nucleon. The constraint may be evaded if there are some new physics effects that give rise to the mass difference between the neutral components to split them into two Majorana fermions. If the mass difference is larger than $\mathcal{O}(100)$ keV, the scatterings with nucleon are not induced by the tree-level Z boson exchange. In what follows, we assume the presence of the mass difference and regard the lighter neutral component χ^0 as a DM candidate. The mass difference is

[8] In the case of the scalar DM, on the other hand, there always exist quartic couplings to the Higgs boson, and the couplings also induce the interactions of the DM with quarks and gluon.

JHEP06(2015)097

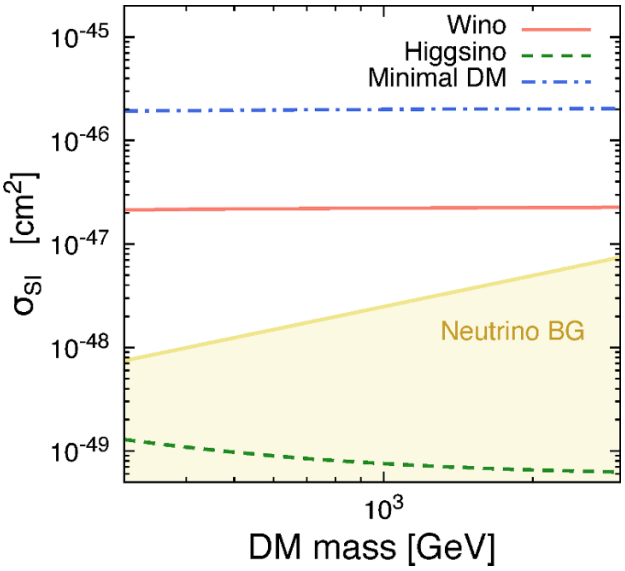

Figure 7. SI scattering cross sections of the $\mathrm{SU}(2)_L$ multiplet DM candidates. Red solid, green dashed, and blue dash-dotted lines correspond to the $(n, Y) = (3, 0)$, $(2, 1/2)$, and $(5, 0)$ cases, respectively. Yellow shaded area indicates the region in which neutrino background overcomes the DM signal [83].

assumed to be small enough to be neglected in the following calculation. In this case, the interactions including the neutral components are given by

$$\begin{aligned}\mathcal{L}_{\mathrm{int}} =& \frac{g_2}{4}\sqrt{n^2-(2Y-1)^2}\,\overline{\chi^+}\not{W}^+\chi^0 + \frac{g_2}{4}\sqrt{n^2-(2Y+1)^2}\,\overline{\chi^0}\not{W}^+\chi^- + \mathrm{h.c.} \\ &+ ig_Z Y\overline{\chi^0}\not{Z}\eta^0 \ . \end{aligned} \tag{4.1}$$

Here n is the number of the components in the DM $\mathrm{SU}(2)_L$ multiplet, $g_Z \equiv \sqrt{g_Y^2 + g_2^2}$ with g_Y the $\mathrm{U}(1)_Y$ gauge coupling constant, and η^0 and Z_μ for the heavier neutral component and the Z boson, respectively.

The LO calculation of the scattering cross section with a nucleon for this type of DM candidates is given in ref. [73]. As in the case of the wino DM, we find that there is a significant cancellation among the contributions to the scattering amplitude. Therefore, the NLO corrections are of importance to evaluate the scattering cross section precisely. We compute the NLO scattering cross section in a similar manner to above discussion. The only difference is the electroweak matching conditions, which we summarize in appendix B. Below the electroweak scale, the procedure is completely the same as before.

In figure 7 we plot the SI scattering cross sections for several $\mathrm{SU}(2)_L$ multiplet DM candidates. Here the red solid, green dashed, and blue dash-dotted lines represent the $(n, Y) = (3, 0)$, $(2, 1/2)$, and $(5, 0)$ cases, respectively. The triplet case corresponds to the wino DM, while the doublet one is regarded as the higgsino DM. The $(n, Y) = (5, 0)$ fermion DM is the so-called minimal DM [108–111], for which the gauge symmetry guarantees its

JHEP06(2015)097

stability. Again, the yellow shaded area indicates the region in which neutrino background overcomes the DM signal [83]. We find that all of the scattering cross sections are almost constant in the mass region we are interested in, as already seen in the case of wino DM. In the heavy DM mass limit, the DM-proton effective coupling $f^p \equiv f^p_{\rm scalar} + f^p_{\rm twist2}$ at the NLO is given by

$$f^p = (n^2 - 4Y^2 - 1) f^p_W + Y^2 f^p_Z \,, \tag{4.2}$$

with

$$\begin{aligned} f^p_W &= 2.9 \times 10^{-11}\ \text{GeV}^{-2} \,, \\ f^p_Z &= -1.8 \times 10^{-10}\ \text{GeV}^{-2} \,, \end{aligned} \tag{4.3}$$

from which one readily obtains the SI scattering cross section for a generic $\mathrm{SU}(2)_L$ DM candidate. It is seen that the $(n, Y) = (3, 0)$ and $(5, 0)$ cases offer the SI scattering cross sections well above the neutrino background, while that of the $(n, Y) = (2, 1/2)$ case falls far below the background. Compared to the previous results in ref. [73], slightly larger SI scattering cross sections are obtained for DM candidates with $Y = 0$. As for the $(n, Y) = (2, 1/2)$ case, on the other hand, we obtain a smaller SI scattering cross section.[9]

5 Conclusion and discussion

In this paper we have completed the calculation of the wino-nucleon scattering cross section up to the NLO in α_s/π. It turns out that the inclusion of the NLO corrections allows us to reduce the theoretical uncertainty significantly, which is now $\mathcal{O}(10)\%$ level. The NLO scattering cross section is larger than the LO one by about 70%. The resultant cross section is well above the neutrino background, and thus the DM direct detection experiment is a promising tool for examining the wino DM scenario. In addition, we give the NLO results for the cases with a generic $\mathrm{SU}(2)_L$ multiplet DM, some of which may also be probed in future experiments.

At present, the uncertainties from the input parameters, especially those of the scalar matrix elements, dominate the theoretical error. If future lattice simulations determine the charm-quark content in nucleon with good accuracy, the uncertainties are to be reduced considerably. We strongly anticipate the developments in the field.

Acknowledgments

We would like to thank Hiroshi Ohki for useful discussions. The work is supported by Grant-in-Aid for Scientific research from the Ministry of Education, Science, Sports, and Culture (MEXT), Japan, No. 24340047 and No. 23104011, (J.H.), Research Fellowships of the Japan Society for the Promotion of Science for Young Scientists (N.N.), and also by World Premier International Research Center Initiative (WPI Initiative), MEXT, Japan (J.H.and N.N.). This work was supported in part by the German Science Foundation (DFG) within the Collaborative Research Center 676 Particles, "Strings and the Early Universe".

[9] Here we note that the Z boson loop contribution in ref. [73] is found to be different from ours by a factor of two.

JHEP06(2015)097

A Mass functions

Here we list the mass functions used in text:

$$g_{\rm H}(x) = 2\sqrt{x}(2 - x\ln x) - \frac{2}{b_x}(2 + 2x - x^2)\tan^{-1}\left(\frac{2b_x}{\sqrt{x}}\right), \tag{A.1}$$

$$g_{\rm B1}(x) = \frac{1}{24}\sqrt{x}(2 - x\ln x) + \frac{1}{24b_x}(4 - 2x + x^2)\tan^{-1}\left(\frac{2b_x}{\sqrt{x}}\right), \tag{A.2}$$

$$\begin{aligned} g_{\rm btm}(x,y) = &- \frac{x^{\frac{3}{2}}y}{12(x-y)^2} - \frac{x^{\frac{5}{2}}y^2}{24(x-y)^3}\ln\left(\frac{x}{y}\right) \\ &- \frac{xy(2y + 6x + 2xy - x^2y)}{24b_x(x-y)^3}\tan^{-1}\left(\frac{2b_x}{\sqrt{x}}\right) \\ &+ \frac{x^{\frac{3}{2}}y^{\frac{1}{2}}(2x + 6y + 2xy - xy^2)}{24b_y(x-y)^3}\tan^{-1}\left(\frac{2b_y}{\sqrt{y}}\right), \end{aligned} \tag{A.3}$$

$$\begin{aligned} g_{\rm top}(x,y) = &\frac{x^{\frac{3}{2}}}{12(x-y)} - \frac{x^{\frac{5}{2}}(x-2y)}{24(x-y)^2}\ln x - \frac{x^{\frac{3}{2}}y^2}{24(x-y)^2}\ln y \\ &+ \frac{x\{x^3 + 4y + 4x(1+y) - 2x^2(1+y)\}}{24b_x(x-y)^2}\tan^{-1}\left(\frac{2b_x}{\sqrt{x}}\right) \\ &- \frac{x^{\frac{3}{2}}y^{\frac{1}{2}}b_y(2+y)}{6(x-y)^2}\tan^{-1}\left(\frac{2b_y}{\sqrt{y}}\right), \end{aligned} \tag{A.4}$$

$$\begin{aligned} g_{\rm T_1}(x,y) = &\frac{x^{\frac{3}{2}}\{x(1-2x) + y(13+2x) - 2y^2\}}{12(x-y)^2} \\ &- \frac{x^{\frac{3}{2}}\{x^3(2-x) + 2xy(3 - 3x + x^2) + 6y^2(2-x)\}}{12(x-y)^3}\ln x \\ &+ \frac{x^{\frac{3}{2}}y\{2x(3 - 6y + y^2) + y(12 + 2y - y^2)\}}{12(x-y)^3}\ln y \\ &+ \frac{x\{4x^2b_x^2(2+x^2) - 2xy(6 - 7x + 5x^2 - x^3) - 6y^2(2 - 4x + x^2)\}}{12b_x(x-y)^3}\tan^{-1}\left(\frac{2b_x}{\sqrt{x}}\right) \\ &- \frac{x^{\frac{3}{2}}y^{\frac{1}{2}}\{2x(3-y)(2 + 5y - y^2) - y(2-y)(14 + 2y - y^2)\}}{12b_y(x-y)^3}\tan^{-1}\left(\frac{2b_y}{\sqrt{y}}\right), \end{aligned} \tag{A.5}$$

$$\begin{aligned} g_{\rm T_2}(x,y) = &\frac{x^{\frac{3}{2}}\{x(-1+2x) - (1+2x)y + 2y^2\}}{4(x-y)^2} \\ &+ \frac{x^{\frac{5}{2}}\{(2-x)x^2 + 2y(1 - 3x + x^2)\}}{4(x-y)^3}\ln x \\ &+ \frac{x^{\frac{3}{2}}y\{y^2(y-2) - 2x(1 - 3y + y^2)\}}{4(x-y)^3}\ln y \\ &+ \frac{x^3\{x(2 - 4x + x^2) - 2y(5 - 5x + x^2)\}}{4b_x(x-y)^3}\tan^{-1}\left(\frac{2b_x}{\sqrt{x}}\right) \\ &+ \frac{x^{\frac{3}{2}}y^{\frac{3}{2}}(2x(5 - 5y + y^2) - y(2 - 4y + y^2))}{4b_y(x-y)^3}\tan^{-1}\left(\frac{2b_y}{\sqrt{y}}\right), \end{aligned} \tag{A.6}$$

JHEP06(2015)097

$$h_{\mathrm{T}_1}(x) = -\frac{\sqrt{x}}{12}\{3-2x-x(3-x)\ln x\} + \frac{1}{3}b_x\, x(1-x)\tan^{-1}\left(\frac{2b_x}{\sqrt{x}}\right), \tag{A.7}$$

$$h_{\mathrm{T}_2}(x) = -\frac{\sqrt{x}}{12}\{1+6x+x(4-3x)\ln x\} + \frac{1}{12b_x}(4-2x+10x^2-3x^3)\tan^{-1}\left(\frac{2b_x}{\sqrt{x}}\right), \tag{A.8}$$

where we have defined $b_x \equiv \sqrt{1-x/4}$. Note that

$$g_{\mathrm{T}_1}(x,0) = \frac{1}{12}\sqrt{x}\{1-2x-x(2-x)\ln x\} + \frac{1}{3}b_x(2+x^2)\tan^{-1}\left(\frac{2b_x}{\sqrt{x}}\right), \tag{A.9}$$

$$g_{\mathrm{T}_2}(x,0) = -\frac{1}{4}\sqrt{x}\{1-2x-x(2-x)\ln x\} + \frac{1}{4b_x}x(2-4x+x^2)\tan^{-1}\left(\frac{2b_x}{\sqrt{x}}\right), \tag{A.10}$$

are equal to $g_{\mathrm{T}_1}(x)$ and $g_{\mathrm{T}_2}(x)$ in ref. [71], respectively. On the other hand, $g^{\log}_{\mathrm{T}_i}(x,y;\mu_W)$ are given by the following integrals:

$$g^{\log}_{\mathrm{T}_i}(x,y;\mu_W) = g^{\mathrm{num}}_{\mathrm{T}_i}(x,y) + \ln\left(x\frac{M^2}{\mu_W^2}\right) g_{\mathrm{T}_i}(x,y), \tag{A.11}$$

with

$$\begin{aligned} g^{\mathrm{num}}_{\mathrm{T}_1}(x,y) =& \frac{x^{\frac{3}{2}}}{24}\int_0^\infty dt\, \frac{1}{(t+x)^2(t+y)^2}\Big[6y\{-4t-t^2+(2+t)\sqrt{t}\sqrt{4+t}\} \\ &+ t\{-6t+4t^2+t^3+(2-t)(4+t)\sqrt{t}\sqrt{4+t}\}\Big]\ln\left(\frac{t}{x}\right), \\ g^{\mathrm{num}}_{\mathrm{T}_2}(x,y) =& \frac{x^{\frac{3}{2}}}{8}\int_0^\infty dt\, \frac{t^2\{-2-4t-t^2+(2+t)\sqrt{t}\sqrt{4+t}\}}{(t+x)^2(t+y)^2}\ln\left(\frac{t}{x}\right). \end{aligned} \tag{A.12}$$

We compute these integrals numerically.

For the generic $\mathrm{SU}(2)_L$ DM case, we further introduce the following functions:

$$\begin{aligned} f_V(x,y) &= f_V^{\mathrm{anl}}(x,y) + f_V^{\mathrm{num}}(x,y), \\ f_A(x,y) &= f_A^{\mathrm{anl}}(x,y) + f_A^{\mathrm{num}}(x,y), \end{aligned} \tag{A.13}$$

JHEP06(2015)097

where

$$
\begin{aligned}
f_V^{\rm anl}(x,y) =& -\frac{\sqrt{x}(x^2-xy+12y^2)}{12(x-4y)^2} \\
&+\frac{x^{\frac{3}{2}}(x^3-12x^2y+20xy^2-48y^3)}{24(x-4y)^3}\ln x+\frac{x^{\frac{3}{2}}y^2(7x-4y)}{6(x-4y)^3}\ln(4y) \\
&+\frac{x^{\frac{3}{2}}y^{\frac{1}{2}}\{5x+28y+2y(7x-4y)(1-2y)\}}{12(x-4y)^3\sqrt{1-y}}\tan^{-1}\left(\frac{\sqrt{1-y}}{\sqrt{y}}\right) \\
&-\frac{4(x^3+44xy^2-48y^3)+x(x-2)(x^3-12x^2y+20xy^2-48y^3)}{24(x-4y)^3b_x}\tan^{-1}\left(\frac{2b_x}{\sqrt{x}}\right),
\end{aligned}
\tag{A.14}
$$

$$
\begin{aligned}
f_A^{\rm anl}(x,y) =& \frac{\sqrt{x}(x-2y)}{4(x-4y)}-\frac{x^{\frac{3}{2}}(x^2-8xy+8y^2)}{8(x-4y)^2}\ln x-\frac{x^{\frac{3}{2}}y^2}{(x-4y)^2}\ln(4y) \\
&+\frac{x^{\frac{3}{2}}\sqrt{y}(2y^2-y-1)}{(x-4y)^2\sqrt{1-y}}\tan^{-1}\left(\frac{\sqrt{1-y}}{\sqrt{y}}\right) \\
&+\frac{4(x^2-2xy+8y^2)+x(x-2)(x^2-8xy+8y^2)}{8(x-4y)^2b_x}\tan^{-1}\left(\frac{2b_x}{\sqrt{x}}\right),
\end{aligned}
\tag{A.15}
$$

while $f_V^{\rm num}(x,y)$ and $f_A^{\rm num}(x,y)$ are expressed by the integral form as

$$
f_V^{\rm num}(x,y) = -x^{\frac{3}{2}}y^2\int_0^\infty dt\frac{(t+2y)\{(2-t)\sqrt{t+4}+t\sqrt{t}\}}{2t(t+x)^2(t+4y)^{\frac{5}{2}}}\ln\left(\frac{\sqrt{t+4y}+\sqrt{t}}{\sqrt{t+4y}-\sqrt{t}}\right), \tag{A.16}
$$

$$
f_V^{\rm num}(x,y) = x^{\frac{3}{2}}y^2\int_0^\infty dt\frac{(t+4y)\{(2-t)\sqrt{t+4}+t\sqrt{t}\}}{2t(t+x)^2(t+4y)^{\frac{5}{2}}}\ln\left(\frac{\sqrt{t+4y}+\sqrt{t}}{\sqrt{t+4y}-\sqrt{t}}\right). \tag{A.17}
$$

Again, these integrals are evaluated numerically. The functions $f_V^{\rm anl}(x,y)$ and $f_A^{\rm anl}(x,y)$ are given by functions in ref. [73] as $f_V^{\rm anl}(x,y) = G_{t1}(x,y)/4$ and $f_A^{\rm anl}(x,y) = G_{t2}(x,y)/4$.

In the large DM mass limit, i.e., $x, y \to 0$ with the ratio y/x fixed, the above analytic functions are reduced to as follows:

$$
g_{\rm H}(x) \to -2\pi\,, \tag{A.18}
$$

$$
g_{\rm B1}(x) \to \frac{\pi}{12}\,, \tag{A.19}
$$

$$
g_{\rm btm}(x,y) \to \frac{\pi}{24}\frac{r}{(1+r)^3}\,, \tag{A.20}
$$

$$
g_{\rm top}(x,y) \to \frac{\pi}{12(1+r)^2}\,, \tag{A.21}
$$

$$
g_{\rm T_1}(x,y) \to \frac{\pi(2+3r)}{6(1+r)^3}\,, \tag{A.22}
$$

$$
g_{\rm T_2}(x,y) \to 0\,, \tag{A.23}
$$

$$
h_{\rm T_1}(x) \to 0\,, \tag{A.24}
$$

$$
h_{\rm T_2}(x) \to \frac{\pi}{6}\,, \tag{A.25}
$$

JHEP06(2015)097

$$g_{\mathrm{T}_1}^{\mathrm{num}}(x,y) \to -\frac{\pi\{(1+r)^2(1-r)(2-3r)+(3-7r^2)r\ln r\}}{3(1-r^2)^3}\,, \tag{A.26}$$

$$g_{\mathrm{T}_2}^{\mathrm{num}}(x,y) \to 0\,, \tag{A.27}$$

$$f_V^{\mathrm{anl}}(x,y) \to \frac{\pi}{24}\frac{(-2+5r+28r^3-88r^4+96r^6)}{(1-4r^2)^3}\,, \tag{A.28}$$

$$f_A^{\mathrm{anl}}(x,y) \to \frac{\pi}{4}\frac{(1-2r-2r^2+8r^4)}{(1-4r^2)^2}\,, \tag{A.29}$$

with $r \equiv \sqrt{y/x}$ and

$$f_V^{\mathrm{num}}(z,\tau) \to -0.189\,, \tag{A.30}$$

$$f_A^{\mathrm{num}}(z,\tau) \to 0.364\,. \tag{A.31}$$

Here we have set the values for the masses of Z boson and top quark in z and τ, respectively.

B Results for the electroweak-interacting DM

In this appendix, we summarize the electroweak matching conditions for generic $\mathrm{SU}(2)_L$ multiplet DM.

B.1 Current correlator

To begin with, we consider the OPEs of the electroweak current correlators as in section 2.3.2. The correlation function of the charged currents has been already discussed there. Here we give the OPEs of the neutral current correlator, for it is necessary to evaluate the Z boson contribution. The correlation function of the weak neutral current is defined by

$$\Pi_{\mu\nu}^Z(q) \equiv i\int d^4x\; e^{iq\cdot x}T\{J_\mu^Z(x)J_\nu^Z(0)^\dagger\}\,, \tag{B.1}$$

where

$$J_\mu^Z = \frac{g_Z}{2}\sum_q \bar{q}\gamma^\mu(g_V^q - g_A^q\gamma^5)q\,, \tag{B.2}$$

with

$$g_V^q \equiv T_{q_L}^3 - 2\sin^2\theta_W Q_q\,, \qquad g_A^q \equiv T_{q_L}^3\,. \tag{B.3}$$

Let us first evaluate the Wilson coefficients of the scalar operators. For the scalar operators, the correlator is decomposed to the transverse and longitudinal parts as

$$\Pi_{\mu\nu}^Z(q)|_{\mathrm{scalar}} = \left(-g_{\mu\nu}+\frac{q_\mu q_\nu}{q^2}\right)\Pi_T^Z(q^2) + \frac{q_\mu q_\nu}{q^2}\Pi_L^Z(q^2)\,. \tag{B.4}$$

Again, only the transverse part is relevant to the calculation. The OPE coefficients are defined by

$$\Pi_T^Z(q^2) = \sum_q c_{Z,S}^q(q^2;\mu_W)m_q\bar{q}q + c_{Z,S}^G(q^2;\mu_W)\frac{\alpha_s}{\pi}G_{\mu\nu}^a G^{a\mu\nu}\,, \tag{B.5}$$

JHEP06(2015)097

are then evaluated as follows [94]:

$$c^q_{Z,S}(q^2;\mu_W) = \frac{g_Z^2}{2q^2}\left[\{(g_V^q)^2-(g_A^q)^2\}+\frac{\alpha_s}{3\pi}\{(g_V^q)^2-7(g_A^q)^2\}\right], \tag{B.6}$$

$$\begin{aligned} c^G_{Z,S}(q^2;\mu_W) =& \sum_q \frac{g_Z^2}{48q^2}\left(1+\frac{7\alpha_s}{6\pi}\right)\{(g_V^q)^2+(g_A^q)^2\} \\ &+ \frac{g_Z^2\{(g_V^t)^2(-q^4+4m_t^2q^2-12m_t^4)+3(g_A^t)^2(q^2-4m_t^2)(q^2-2m_t^2)\}}{48q^2(q^2-4m_t^2)^2} \\ &+ \frac{g_Z^2m_t^4\{(g_V^t)^2(q^2-2m_t^2)-(g_A^t)^2(q^2-4m_t^2)\}\sqrt{1-\frac{4m_t^2}{q^2}}\ \ln\left(\frac{\sqrt{1-\frac{4m_t^2}{q^2}}+1}{\sqrt{1-\frac{4m_t^2}{q^2}}-1}\right)}{4q^2(q^2-4m_t^2)^3}, \end{aligned} \tag{B.7}$$

with $q = u, d, s, c, b$. Here we drop the NLO contribution of top quark for simplicity. This contribution is also readily obtained from the results in ref. [94]. The LO terms in the above equations agree with the results given in ref. [73].

Next, we consider the twist-2 operators. Their contribution to the correlation function is written as [95]

$$\begin{aligned} \Pi^Z_{\mu\nu}(q)|_{\text{twist2}} = g_Z^2\sum_{i=q,G}\Bigg[&-\left(\frac{g_{\mu\rho}g_{\nu\sigma}q^2-g_{\mu\rho}q_\nu q_\sigma-q_\mu q_\rho g_{\nu\sigma}+g_{\mu\nu}q_\rho q_\sigma}{(q^2)^2}\right)c^i_{Z,2} \\ &+\left(g_{\mu\nu}-\frac{q_\mu q_\nu}{q^2}\right)\frac{q_\rho q_\sigma}{(q^2)^2}c^i_{Z,L}\Bigg]\mathcal{O}^{i\rho\sigma}, \end{aligned} \tag{B.8}$$

with the coefficients given by

$$\begin{aligned} c^q_{Z,2}(\mu_W) &= [(g_V^q)^2+(g_A^q)^2]\left\{1+\frac{\alpha_s(\mu_W)}{4\pi}\left[-\frac{1}{2}\left(\frac{64}{9}\right)\ln\left(\frac{-q^2}{\mu_W^2}\right)+\frac{4}{9}\right]\right\}, \\ c^q_{Z,L}(\mu_W) &= [(g_V^q)^2+(g_A^q)^2]\left\{\frac{\alpha_s(\mu_W)}{4\pi}\left[\frac{16}{9}\right]\right\}, \\ c^G_{Z,2}(\mu_W) &= \sum_{q=u,d,s,c,b}[(g_V^q)^2+(g_A^q)^2]\left\{\frac{\alpha_s(\mu_W)}{4\pi}\left[-\frac{1}{2}\left(\frac{4}{3}\right)\ln\left(\frac{-q^2}{\mu_W^2}\right)+\frac{1}{2}\right]\right\}, \\ c^G_{Z,L}(\mu_W) &= \sum_{q=u,d,s,c,b}[(g_V^q)^2+(g_A^q)^2]\left\{\frac{\alpha_s(\mu_W)}{4\pi}\left[-\frac{2}{3}\right]\right\}. \end{aligned} \tag{B.9}$$

Here again, we have neglected the top-quark contribution to the NLO gluon coefficients.

JHEP06(2015)097

B.2 Wilson coefficients

Now we calculate the electroweak-scale matching conditions. For the scalar-type quark operators, we have

$$\begin{aligned} C_{\rm S}^q(\mu_W) =& \frac{\alpha_2^2}{4m_h^2}\left[\frac{n^2-(4Y^2+1)}{8m_W}g_{\rm H}(w)+\frac{Y^2}{2m_Z\cos^4\theta_W}g_{\rm H}(z)\right] \\ &+\frac{\alpha_2^2}{m_W^3}\frac{n^2-(4Y^2+1)}{8}\frac{\alpha_s(\mu_W)}{4\pi}[-12g_{\rm B1}(w)] \\ &+\frac{\alpha_2^2Y^2}{\cos^4\theta_W m_Z^3}\left[\{(g_V^q)^2-(g_A^q)^2\}+\frac{\alpha_s}{3\pi}\{(g_V^q)^2-7(g_A^q)^2\}\right][3g_{\rm B1}(z)]\,, \end{aligned} \tag{B.10}$$

for $q=u,d,s,c$, and

$$\begin{aligned} C_{\rm S}^b(\mu_W) =& \frac{\alpha_2^2}{4m_h^2}\left[\frac{n^2-(4Y^2+1)}{8m_W}g_{\rm H}(w)+\frac{Y^2}{2m_Z\cos^4\theta_W}g_{\rm H}(z)\right] \\ &+\frac{\alpha_2^2}{m_W^3}\frac{n^2-(4Y^2+1)}{8}[(-3)g_{\rm btm}(w,\tau)] \\ &+\frac{\alpha_2^2Y^2}{\cos^4\theta_W m_Z^3}\left[\{(g_V^q)^2-(g_A^q)^2\}+\frac{\alpha_s}{3\pi}\{(g_V^q)^2-7(g_A^q)^2\}\right][3g_{\rm B1}(z)]\,, \end{aligned} \tag{B.11}$$

where θ_W is the weak mixing angle and $z\equiv m_Z^2/M^2$.[10] The Wilson coefficient of the scalar-type gluon operator is, on the other hand, computed as

$$\begin{aligned} C_{\rm S}^G(\mu_W) =& -\frac{\alpha_2^2}{48m_h^2}\left[1+\frac{11}{4\pi}\alpha_s(\mu_W)\right]\left[\frac{n^2-(4Y^2+1)}{8m_W}g_{\rm H}(w)+\frac{Y^2}{2m_Z\cos^4\theta_W}g_{\rm H}(z)\right] \\ &+\frac{\alpha_2^2}{4m_W^3}\frac{n^2-(4Y^2+1)}{8}\left[\left(2+\frac{7}{3}\frac{\alpha_s(\mu_W)}{\pi}\right)g_{\rm B1}(w)+g_{\rm top}(w,\tau)\right] \\ &+\frac{\alpha_2^2Y^2}{8\cos^4\theta_W m_Z^3}\left[\sum_{q=u,d,s,c,b}\left(1+\frac{7\alpha_s}{6\pi}\right)\{(g_V^q)^2+(g_A^q)^2\}g_{\rm B1}(z)\right. \\ &\left.+(g_V^t)^2 f_V(z,\tau)+(g_A^t)^2 f_A(z,\tau)\right]\,, \end{aligned} \tag{B.12}$$

where the functions $f_V(x,y)$ and $f_A(x,y)$ are given in appendix A. The twist-2 contribution is given by

$$\begin{aligned} C_{{\rm T}_i}^q(\mu_W) =& \frac{\alpha_2^2}{m_W^3}\frac{n^2-(4Y^2+1)}{8}\left[g_{{\rm T}_i}(w,0)\right. \\ &\left.+\frac{\alpha_s(\mu_W)}{4\pi}\left(-\frac{32}{9}g_{{\rm T}_i}^{\log}(w,0;\mu_W)+\frac{9}{4}g_{{\rm T}_i}(w,0)+\frac{16}{9}h_{{\rm T}_i}(w)\right)\right] \\ &+\frac{\alpha_2^2Y^2\{(g_V^q)^2+(g_A^q)^2\}}{m_Z^3\cos^4\theta_W}\left[g_{{\rm T}_i}(z,0)\right. \\ &\left.+\frac{\alpha_s(\mu_W)}{4\pi}\left(-\frac{32}{9}g_{{\rm T}_i}^{\log}(z,0;\mu_W)+\frac{9}{4}g_{{\rm T}_i}(z,0)+\frac{16}{9}h_{{\rm T}_i}(z)\right)\right]\,, \end{aligned} \tag{B.13}$$

[10] Note that $g_{\rm S}(x)$ in ref. [73] is equal to $6g_{\rm B1}(x)$.

JHEP06(2015)097

for $q = u, d, s, c$,

$$C^b_{\mathrm{T}_i}(\mu_W) = \frac{\alpha_2^2}{m_W^3}\frac{n^2-(4Y^2+1)}{8}\left[g_{\mathrm{T}_i}(w,\tau)+\frac{\alpha_s(\mu_W)}{4\pi}\left(-\frac{32}{9}g^{\log}_{\mathrm{T}_i}(w,\tau;\mu_W)\right)\right] + \frac{\alpha_2^2 Y^2\{(g_V^b)^2+(g_A^b)^2\}}{m_Z^3\cos^4\theta_W}\left[g_{\mathrm{T}_i}(z,0) + \frac{\alpha_s(\mu_W)}{4\pi}\left(-\frac{32}{9}g^{\log}_{\mathrm{T}_i}(z,0;\mu_W)+\frac{9}{4}g_{\mathrm{T}_i}(z,0)+\frac{16}{9}h_{\mathrm{T}_i}(z)\right)\right], \tag{B.14}$$

and

$$C^G_{\mathrm{T}_i}(\mu_W) = \frac{\alpha_2^2}{m_W^3}\frac{n^2-(4Y^2+1)}{8}\frac{\alpha_s(\mu_W)}{4\pi}\times \left[4\times\left(-\frac{2}{3}g^{\log}_{\mathrm{T}_i}(w,0;\mu_W)+\frac{1}{2}g_{\mathrm{T}_i}(w,0)-\frac{2}{3}h_{\mathrm{T}_i}(w)\right)-\frac{2}{3}g^{\log}_{\mathrm{T}_i}(w,\tau;\mu_W)\right] + \sum_{q=u,d,s,c,b}\frac{\alpha_2^2 Y^2\{(g_V^q)^2+(g_A^q)^2\}}{m_Z^3\cos^4\theta_W}\frac{\alpha_s(\mu_W)}{4\pi}\left[-\frac{2}{3}g^{\log}_{\mathrm{T}_i}(z,0;\mu_W)+\frac{1}{2}g_{\mathrm{T}_i}(z,0)-\frac{2}{3}h_{\mathrm{T}_i}(z)\right]. \tag{B.15}$$

Here we note that the LO Z boson contribution to C^q_{S}, C^G_{S}, and $C^q_{\mathrm{T}_i}$ differs from that given in ref. [73] by a factor of two.

References

[1] CMS collaboration, *Search for new physics in the multijet and missing transverse momentum final state in proton-proton collisions at $\sqrt{s}$= 8 TeV*, *JHEP* **06** (2014) 055 [arXiv:1402.4770] [INSPIRE].

[2] ATLAS collaboration, *Search for squarks and gluinos with the ATLAS detector in final states with jets and missing transverse momentum using $\sqrt{s} = 8$ TeV proton–proton collision data*, *JHEP* **09** (2014) 176 [arXiv:1405.7875] [INSPIRE].

[3] I. Affleck, M. Dine and N. Seiberg, *Supersymmetry Breaking by Instantons*, *Phys. Rev. Lett.* **51** (1983) 1026 [INSPIRE].

[4] I. Affleck, M. Dine and N. Seiberg, *Dynamical Supersymmetry Breaking in Supersymmetric QCD*, *Nucl. Phys.* **B 241** (1984) 493 [INSPIRE].

[5] I. Affleck, M. Dine and N. Seiberg, *Dynamical Supersymmetry Breaking in Chiral Theories*, *Phys. Lett.* **B 137** (1984) 187 [INSPIRE].

[6] I. Affleck, M. Dine and N. Seiberg, *Dynamical Supersymmetry Breaking in Four-Dimensions and its Phenomenological Implications*, *Nucl. Phys.* **B 256** (1985) 557 [INSPIRE].

[7] I. Affleck, M. Dine and N. Seiberg, *Calculable Nonperturbative Supersymmetry Breaking*, *Phys. Rev. Lett.* **52** (1984) 1677 [INSPIRE].

JHEP06(2015)097

[8] I. Affleck, M. Dine and N. Seiberg, *Exponential Hierarchy From Dynamical Supersymmetry Breaking*, *Phys. Lett.* **B 140** (1984) 59 [INSPIRE].

[9] L. Randall and R. Sundrum, *Out of this world supersymmetry breaking*, *Nucl. Phys.* **B 557** (1999) 79 [hep-th/9810155] [INSPIRE].

[10] G.F. Giudice, M.A. Luty, H. Murayama and R. Rattazzi, *Gaugino mass without singlets*, *JHEP* **12** (1998) 027 [hep-ph/9810442] [INSPIRE].

[11] J. Hisano, S. Matsumoto, M. Nagai, O. Saito and M. Senami, *Non-perturbative effect on thermal relic abundance of dark matter*, *Phys. Lett.* **B 646** (2007) 34 [hep-ph/0610249] [INSPIRE].

[12] T. Gherghetta, G.F. Giudice and J.D. Wells, *Phenomenological consequences of supersymmetry with anomaly induced masses*, *Nucl. Phys.* **B 559** (1999) 27 [hep-ph/9904378] [INSPIRE].

[13] T. Moroi and L. Randall, *Wino cold dark matter from anomaly mediated SUSY breaking*, *Nucl. Phys.* **B 570** (2000) 455 [hep-ph/9906527] [INSPIRE].

[14] J.D. Wells, *Implications of supersymmetry breaking with a little hierarchy between gauginos and scalars*, hep-ph/0306127 [INSPIRE].

[15] N. Arkani-Hamed and S. Dimopoulos, *Supersymmetric unification without low energy supersymmetry and signatures for fine-tuning at the LHC*, *JHEP* **06** (2005) 073 [hep-th/0405159] [INSPIRE].

[16] G.F. Giudice and A. Romanino, *Split supersymmetry*, *Nucl. Phys.* **B 699** (2004) 65 [hep-ph/0406088] [INSPIRE].

[17] N. Arkani-Hamed, S. Dimopoulos, G.F. Giudice and A. Romanino, *Aspects of split supersymmetry*, *Nucl. Phys.* **B 709** (2005) 3 [hep-ph/0409232] [INSPIRE].

[18] J.D. Wells, *PeV-scale supersymmetry*, *Phys. Rev.* **D 71** (2005) 015013 [hep-ph/0411041] [INSPIRE].

[19] G.F. Giudice and A. Strumia, *Probing High-Scale and Split Supersymmetry with Higgs Mass Measurements*, *Nucl. Phys.* **B 858** (2012) 63 [arXiv:1108.6077] [INSPIRE].

[20] L.J. Hall and Y. Nomura, *Spread Supersymmetry*, *JHEP* **01** (2012) 082 [arXiv:1111.4519] [INSPIRE].

[21] M. Ibe and T.T. Yanagida, *The Lightest Higgs Boson Mass in Pure Gravity Mediation Model*, *Phys. Lett.* **B 709** (2012) 374 [arXiv:1112.2462] [INSPIRE].

[22] M. Ibe, S. Matsumoto and T.T. Yanagida, *Pure Gravity Mediation with* $m_{3/2} =$ *10-100TeV*, *Phys. Rev.* **D 85** (2012) 095011 [arXiv:1202.2253] [INSPIRE].

[23] A. Arvanitaki, N. Craig, S. Dimopoulos and G. Villadoro, *Mini-Split*, *JHEP* **02** (2013) 126 [arXiv:1210.0555] [INSPIRE].

[24] L.J. Hall, Y. Nomura and S. Shirai, *Spread Supersymmetry with Wino LSP: Gluino and Dark Matter Signals*, *JHEP* **01** (2013) 036 [arXiv:1210.2395] [INSPIRE].

[25] N. Arkani-Hamed, A. Gupta, D.E. Kaplan, N. Weiner and T. Zorawski, *Simply Unnatural Supersymmetry*, arXiv:1212.6971 [INSPIRE].

[26] J.L. Evans, M. Ibe, K.A. Olive and T.T. Yanagida, *Universality in Pure Gravity Mediation*, *Eur. Phys. J.* **C 73** (2013) 2468 [arXiv:1302.5346] [INSPIRE].

JHEP06(2015)097

[27] J.L. Evans, K.A. Olive, M. Ibe and T.T. Yanagida, *Non-Universalities in Pure Gravity Mediation*, *Eur. Phys. J.* **C 73** (2013) 2611 [arXiv:1305.7461] [INSPIRE].

[28] E. Bagnaschi, G.F. Giudice, P. Slavich and A. Strumia, *Higgs Mass and Unnatural Supersymmetry*, *JHEP* **09** (2014) 092 [arXiv:1407.4081] [INSPIRE].

[29] ATLAS collaboration, *Observation of a new particle in the search for the Standard Model Higgs boson with the ATLAS detector at the LHC*, *Phys. Lett.* **B 716** (2012) 1 [arXiv:1207.7214] [INSPIRE].

[30] CMS collaboration, *Observation of a new boson at a mass of 125 GeV with the CMS experiment at the LHC*, *Phys. Lett.* **B 716** (2012) 30 [arXiv:1207.7235] [INSPIRE].

[31] F. Gabbiani, E. Gabrielli, A. Masiero and L. Silvestrini, *A Complete analysis of FCNC and CP constraints in general SUSY extensions of the standard model*, *Nucl. Phys.* **B 477** (1996) 321 [hep-ph/9604387] [INSPIRE].

[32] T. Moroi and M. Nagai, *Probing Supersymmetric Model with Heavy Sfermions Using Leptonic Flavor and CP-violations*, *Phys. Lett.* **B 723** (2013) 107 [arXiv:1303.0668] [INSPIRE].

[33] D. McKeen, M. Pospelov and A. Ritz, *Electric dipole moment signatures of PeV-scale superpartners*, *Phys. Rev.* **D 87** (2013) 113002 [arXiv:1303.1172] [INSPIRE].

[34] W. Altmannshofer, R. Harnik and J. Zupan, *Low Energy Probes of PeV Scale Sfermions*, *JHEP* **11** (2013) 202 [arXiv:1308.3653] [INSPIRE].

[35] K. Fuyuto, J. Hisano, N. Nagata and K. Tsumura, *QCD Corrections to Quark (Chromo)Electric Dipole Moments in High-scale Supersymmetry*, *JHEP* **12** (2013) 010 [arXiv:1308.6493] [INSPIRE].

[36] M. Tanimoto and K. Yamamoto, *Probing the high scale SUSY in CP-violations of K, B^0 and B_s mesons*, *Phys. Lett.* **B 735** (2014) 426 [arXiv:1404.0520] [INSPIRE].

[37] M. Tanimoto and K. Yamamoto, *$K_L \to \pi^0 \nu\bar{\nu}$ decay correlating with ϵ_K in high-scale SUSY*, arXiv:1503.06270 [INSPIRE].

[38] M. Liu and P. Nath, *Higgs boson mass, proton decay, naturalness and constraints of the LHC and Planck data*, *Phys. Rev.* **D 87** (2013) 095012 [arXiv:1303.7472] [INSPIRE].

[39] J. Hisano, D. Kobayashi, T. Kuwahara and N. Nagata, *Decoupling Can Revive Minimal Supersymmetric* SU(5), *JHEP* **07** (2013) 038 [arXiv:1304.3651] [INSPIRE].

[40] M. Dine, P. Draper and W. Shepherd, *Proton decay at M_{pl} and the scale of SUSY-breaking*, *JHEP* **02** (2014) 027 [arXiv:1308.0274] [INSPIRE].

[41] N. Nagata and S. Shirai, *Sfermion Flavor and Proton Decay in High-Scale Supersymmetry*, *JHEP* **03** (2014) 049 [arXiv:1312.7854] [INSPIRE].

[42] J.L. Evans, N. Nagata and K.A. Olive, SU(5) *Grand Unification in Pure Gravity Mediation*, *Phys. Rev.* **D 91** (2015) 055027 [arXiv:1502.00034] [INSPIRE].

[43] S. Weinberg, *Cosmological Constraints on the Scale of Supersymmetry Breaking*, *Phys. Rev. Lett.* **48** (1982) 1303 [INSPIRE].

[44] T. Moroi, M. Yamaguchi and T. Yanagida, *On the solution to the Polonyi problem with 0 (10 TeV) gravitino mass in supergravity*, *Phys. Lett.* **B 342** (1995) 105 [hep-ph/9409367] [INSPIRE].

JHEP06(2015)097

[45] M. Kawasaki, K. Kohri, T. Moroi and A. Yotsuyanagi, *Big-Bang Nucleosynthesis and Gravitino*, *Phys. Rev.* **D 78** (2008) 065011 [arXiv:0804.3745] [INSPIRE].

[46] J. Hisano, T. Kuwahara and N. Nagata, *Grand Unification in High-scale Supersymmetry*, *Phys. Lett.* **B 723** (2013) 324 [arXiv:1304.0343] [INSPIRE].

[47] ATLAS collaboration, *Search for charginos nearly mass degenerate with the lightest neutralino based on a disappearing-track signature in pp collisions at $\sqrt{s} = 8$ TeV with the ATLAS detector*, *Phys. Rev.* **D 88** (2013) 112006 [arXiv:1310.3675] [INSPIRE].

[48] K. Shingo, *Search for Charginos Nearly Mass-Degenerate with the Lightest Neutralino Based on a Disappearing-Track Signature in pp Collisions at $\sqrt{s} = 8$ TeV*, CERN-THESIS-2014-163 (2014).

[49] M. Low and L.-T. Wang, *Neutralino dark matter at 14 TeV and 100 TeV*, *JHEP* **08** (2014) 161 [arXiv:1404.0682] [INSPIRE].

[50] M. Cirelli, F. Sala and M. Taoso, *Wino-like Minimal Dark Matter and future colliders*, *JHEP* **10** (2014) 033 [arXiv:1407.7058] [INSPIRE].

[51] S. Gori, S. Jung, L.-T. Wang and J.D. Wells, *Prospects for Electroweakino Discovery at a 100 TeV Hadron Collider*, *JHEP* **12** (2014) 108 [arXiv:1410.6287] [INSPIRE].

[52] J. Bramante et al., *Relic neutralino surface at a 100 TeV collider*, *Phys. Rev.* **D 91** (2015) 054015 [arXiv:1412.4789] [INSPIRE].

[53] G.G. di Cortona, *Hunting electroweakinos at future hadron colliders and direct detection experiments*, *JHEP* **05** (2015) 035 [arXiv:1412.5952] [INSPIRE].

[54] H. Beauchesne, K. Earl and T. Gregoire, *LHC constraints on Mini-Split anomaly and gauge mediation and prospects for a future 100 TeV pp collider*, arXiv:1503.03099 [INSPIRE].

[55] J. Hisano, S. Matsumoto and M.M. Nojiri, *Explosive dark matter annihilation*, *Phys. Rev. Lett.* **92** (2004) 031303 [hep-ph/0307216] [INSPIRE].

[56] J. Hisano, S. Matsumoto, M.M. Nojiri and O. Saito, *Non-perturbative effect on dark matter annihilation and gamma ray signature from galactic center*, *Phys. Rev.* **D 71** (2005) 063528 [hep-ph/0412403] [INSPIRE].

[57] B. Bhattacherjee, M. Ibe, K. Ichikawa, S. Matsumoto and K. Nishiyama, *Wino Dark Matter and Future dSph Observations*, *JHEP* **07** (2014) 080 [arXiv:1405.4914] [INSPIRE].

[58] FERMI-LAT collaboration, M. Ackermann et al., *Dark matter constraints from observations of 25 Milky Way satellite galaxies with the Fermi Large Area Telescope*, *Phys. Rev.* **D 89** (2014) 042001 [arXiv:1310.0828] [INSPIRE].

[59] A.X. Gonzalez-Morales, S. Profumo and F.S. Queiroz, *Effect of Black Holes in Local Dwarf Spheroidal Galaxies on Gamma-Ray Constraints on Dark Matter Annihilation*, *Phys. Rev.* **D 90** (2014) 103508 [arXiv:1406.2424] [INSPIRE].

[60] HESS collaboration, A. Abramowski et al., *Search for Photon-Linelike Signatures from Dark Matter Annihilations with H.E.S.S.*, *Phys. Rev. Lett.* **110** (2013) 041301 [arXiv:1301.1173] [INSPIRE].

[61] T. Cohen, M. Lisanti, A. Pierce and T.R. Slatyer, *Wino Dark Matter Under Siege*, *JCAP* **10** (2013) 061 [arXiv:1307.4082] [INSPIRE].

[62] J. Fan and M. Reece, *In Wino Veritas? Indirect Searches Shed Light on Neutralino Dark Matter*, *JHEP* **10** (2013) 124 [arXiv:1307.4400] [INSPIRE].

JHEP06(2015)097

[63] A. Hryczuk, I. Cholis, R. Iengo, M. Tavakoli and P. Ullio, *Indirect Detection Analysis: Wino Dark Matter Case Study*, *JCAP* **07** (2014) 031 [arXiv:1401.6212] [INSPIRE].

[64] M. Baumgart, I.Z. Rothstein and V. Vaidya, *Calculating the Annihilation Rate of Weakly Interacting Massive Particles*, *Phys. Rev. Lett.* **114** (2015) 211301 [arXiv:1409.4415] [INSPIRE].

[65] M. Bauer, T. Cohen, R.J. Hill and M.P. Solon, *Soft Collinear Effective Theory for Heavy WIMP Annihilation*, *JHEP* **01** (2015) 099 [arXiv:1409.7392] [INSPIRE].

[66] G. Ovanesyan, T.R. Slatyer and I.W. Stewart, *Heavy Dark Matter Annihilation from Effective Field Theory*, *Phys. Rev. Lett.* **114** (2015) 211302 [arXiv:1409.8294] [INSPIRE].

[67] M. Beneke, C. Hellmann and P. Ruiz-Femenia, *Non-relativistic pair annihilation of nearly mass degenerate neutralinos and charginos III. Computation of the Sommerfeld enhancements*, *JHEP* **05** (2015) 115 [arXiv:1411.6924] [INSPIRE].

[68] M. Baumgart, I.Z. Rothstein and V. Vaidya, *Constraints on Galactic Wino Densities from Gamma Ray Lines*, *JHEP* **04** (2015) 106 [arXiv:1412.8698] [INSPIRE].

[69] LUX collaboration, D.S. Akerib et al., *First results from the LUX dark matter experiment at the Sanford Underground Research Facility*, *Phys. Rev. Lett.* **112** (2014) 091303 [arXiv:1310.8214] [INSPIRE].

[70] J. Hisano, S. Matsumoto, M.M. Nojiri and O. Saito, *Direct detection of the Wino and Higgsino-like neutralino dark matters at one-loop level*, *Phys. Rev.* **D 71** (2005) 015007 [hep-ph/0407168] [INSPIRE].

[71] J. Hisano, K. Ishiwata and N. Nagata, *A complete calculation for direct detection of Wino dark matter*, *Phys. Lett.* **B 690** (2010) 311 [arXiv:1004.4090] [INSPIRE].

[72] J. Hisano, K. Ishiwata and N. Nagata, *Gluon contribution to the dark matter direct detection*, *Phys. Rev.* **D 82** (2010) 115007 [arXiv:1007.2601] [INSPIRE].

[73] J. Hisano, K. Ishiwata, N. Nagata and T. Takesako, *Direct Detection of Electroweak-Interacting Dark Matter*, *JHEP* **07** (2011) 005 [arXiv:1104.0228] [INSPIRE].

[74] J. Hisano, K. Ishiwata and N. Nagata, *Direct Search of Dark Matter in High-Scale Supersymmetry*, *Phys. Rev.* **D 87** (2013) 035020 [arXiv:1210.5985] [INSPIRE].

[75] J.-J. Cao, W.-Y. Wang and J.M. Yang, *Split-SUSY dark matter in light of direct detection limits*, *Phys. Lett.* **B 706** (2011) 72 [arXiv:1108.2834] [INSPIRE].

[76] A. Dedes and D. Karamitros, *Doublet-Triplet Fermionic Dark Matter*, *Phys. Rev.* **D 89** (2014) 115002 [arXiv:1403.7744] [INSPIRE].

[77] K. Cheung, R. Huo, J.S. Lee and Y.-L. Sming Tsai, *Dark Matter in Split SUSY with Intermediate Higgses*, *JHEP* **04** (2015) 151 [arXiv:1411.7329] [INSPIRE].

[78] G.G. di Cortona, *Hunting electroweakinos at future hadron colliders and direct detection experiments*, *JHEP* **05** (2015) 035 [arXiv:1412.5952] [INSPIRE].

[79] R.J. Hill and M.P. Solon, *Universal behavior in the scattering of heavy, weakly interacting dark matter on nuclear targets*, *Phys. Lett.* **B 707** (2012) 539 [arXiv:1111.0016] [INSPIRE].

[80] R.J. Hill and M.P. Solon, *WIMP-nucleon scattering with heavy WIMP effective theory*, *Phys. Rev. Lett.* **112** (2014) 211602 [arXiv:1309.4092] [INSPIRE].

[81] R.J. Hill and M.P. Solon, *Standard Model anatomy of WIMP dark matter direct detection I: weak-scale matching*, *Phys. Rev.* **D 91** (2015) 043504 [arXiv:1401.3339] [INSPIRE].

JHEP06(2015)097

[82] R.J. Hill and M.P. Solon, *Standard Model anatomy of WIMP dark matter direct detection II: QCD analysis and hadronic matrix elements*, *Phys. Rev.* **D 91** (2015) 043505 [arXiv:1409.8290] [INSPIRE].

[83] J. Billard, L. Strigari and E. Figueroa-Feliciano, *Implication of neutrino backgrounds on the reach of next generation dark matter direct detection experiments*, *Phys. Rev.* **D 89** (2014) 023524 [arXiv:1307.5458] [INSPIRE].

[84] M. Drees and M. Nojiri, *Neutralino - nucleon scattering revisited*, *Phys. Rev.* **D 48** (1993) 3483 [hep-ph/9307208] [INSPIRE].

[85] A.J. Buras, *Asymptotic Freedom in Deep Inelastic Processes in the Leading Order and Beyond*, *Rev. Mod. Phys.* **52** (1980) 199 [INSPIRE].

[86] H.D. Politzer, *Power Corrections at Short Distances*, *Nucl. Phys.* **B 172** (1980) 349 [INSPIRE].

[87] C. Arzt, *Reduced effective Lagrangians*, *Phys. Lett.* **B 342** (1995) 189 [hep-ph/9304230] [INSPIRE].

[88] J. Hisano, R. Nagai and N. Nagata, *Effective Theories for Dark Matter Nucleon Scattering*, *JHEP* **05** (2015) 037 [arXiv:1502.02244] [INSPIRE].

[89] R.D. Young and A.W. Thomas, *Octet baryon masses and sigma terms from an* SU(3) *chiral extrapolation*, *Phys. Rev.* **D 81** (2010) 014503 [arXiv:0901.3310] [INSPIRE].

[90] JLQCD collaboration, H. Ohki et al., *Nucleon strange quark content from $N_f = 2 + 1$ lattice QCD with exact chiral symmetry*, *Phys. Rev.* **D 87** (2013) 034509 [arXiv:1208.4185] [INSPIRE].

[91] M.A. Shifman, A.I. Vainshtein and V.I. Zakharov, *Remarks on Higgs Boson Interactions with Nucleons*, *Phys. Lett.* **B 78** (1978) 443 [INSPIRE].

[92] J.F. Owens, A. Accardi and W. Melnitchouk, *Global parton distributions with nuclear and finite-Q^2 corrections*, *Phys. Rev.* **D 87** (2013) 094012 [arXiv:1212.1702] [INSPIRE].

[93] M. Ibe, S. Matsumoto and R. Sato, *Mass Splitting between Charged and Neutral Winos at Two-Loop Level*, *Phys. Lett.* **B 721** (2013) 252 [arXiv:1212.5989] [INSPIRE].

[94] D.J. Broadhurst et al., *Two loop gluon condensate contributions to heavy quark current correlators: Exact results and approximations*, *Phys. Lett.* **B 329** (1994) 103 [hep-ph/9403274] [INSPIRE].

[95] W.A. Bardeen, A.J. Buras, D.W. Duke and T. Muta, *Deep Inelastic Scattering Beyond the Leading Order in Asymptotically Free Gauge Theories*, *Phys. Rev.* **D 18** (1978) 3998 [INSPIRE].

[96] T. Inami, T. Kubota and Y. Okada, *Effective Gauge Theory and the Effect of Heavy Quarks in Higgs Boson Decays*, *Z. Phys.* **C 18** (1983) 69 [INSPIRE].

[97] A. Djouadi and M. Drees, *QCD corrections to neutralino nucleon scattering*, *Phys. Lett.* **B 484** (2000) 183 [hep-ph/0004205] [INSPIRE].

[98] L. Vecchi, *WIMPs and Un-Naturalness*, arXiv:1312.5695 [INSPIRE].

[99] E.G. Floratos, D.A. Ross and C.T. Sachrajda, *Higher Order Effects in Asymptotically Free Gauge Theories. 2. Flavor Singlet Wilson Operators and Coefficient Functions*, *Nucl. Phys.* **B 152** (1979) 493 [INSPIRE].

JHEP06(2015)097

[100] A. Gonzalez-Arroyo and C. Lopez, *Second Order Contributions to the Structure Functions in Deep Inelastic Scattering. 3. The Singlet Case*, *Nucl. Phys.* **B 166** (1980) 429 [INSPIRE].

[101] P.L. Cho and E.H. Simmons, *Searching for G3 in $t\bar{t}$ production*, *Phys. Rev.* **D 51** (1995) 2360 [hep-ph/9408206] [INSPIRE].

[102] PARTICLE DATA GROUP collaboration, K.A. Olive et al., *Review of Particle Physics*, *Chin. Phys.* **C 38** (2014) 090001.

[103] ATLAS collaboration, *Measurement of the Higgs boson mass from the $H \to \gamma\gamma$ and $H \to ZZ^* \to 4\ell$ channels with the ATLAS detector using 25 fb^{-1} of pp collision data*, *Phys. Rev.* **D 90** (2014) 052004 [arXiv:1406.3827] [INSPIRE].

[104] CMS collaboration, *Observation of the diphoton decay of the Higgs boson and measurement of its properties*, *Eur. Phys. J.* **C 74** (2014) 3076 [arXiv:1407.0558] [INSPIRE].

[105] ATLAS, CDF, CMS, D0 collaboration, *First combination of Tevatron and LHC measurements of the top-quark mass*, arXiv:1403.4427 [INSPIRE].

[106] K.G. Chetyrkin, B.A. Kniehl and M. Steinhauser, *Decoupling relations to O (alpha-s^3) and their connection to low-energy theorems*, *Nucl. Phys.* **B 510** (1998) 61 [hep-ph/9708255] [INSPIRE].

[107] ETM collaboration, S. Dinter et al., *Sigma terms and strangeness content of the nucleon with $N_f = 2 + 1 + 1$ twisted mass fermions*, *JHEP* **08** (2012) 037 [arXiv:1202.1480] [INSPIRE].

[108] M. Cirelli, N. Fornengo and A. Strumia, *Minimal dark matter*, *Nucl. Phys.* **B 753** (2006) 178 [hep-ph/0512090] [INSPIRE].

[109] M. Cirelli, A. Strumia and M. Tamburini, *Cosmology and Astrophysics of Minimal Dark Matter*, *Nucl. Phys.* **B 787** (2007) 152 [arXiv:0706.4071] [INSPIRE].

[110] M. Cirelli and A. Strumia, *Minimal Dark Matter: Model and results*, *New J. Phys.* **11** (2009) 105005 [arXiv:0903.3381] [INSPIRE].

[111] M. Farina, D. Pappadopulo and A. Strumia, *A modified naturalness principle and its experimental tests*, *JHEP* **08** (2013) 022 [arXiv:1303.7244] [INSPIRE].

[112] R. Essig, *Direct Detection of Non-Chiral Dark Matter*, *Phys. Rev.* **D 78** (2008) 015004 [arXiv:0710.1668] [INSPIRE].

[113] T. Hambye, F.-S. Ling, L. Lopez Honorez and J. Rocher, *Scalar Multiplet Dark Matter*, *JHEP* **07** (2009) 090 [arXiv:0903.4010] [INSPIRE].

[114] F.S. Queiroz, K. Sinha and A. Strumia, *Leptoquarks, Dark Matter and Anomalous LHC Events*, *Phys. Rev.* **D 91** (2015) 035006 [arXiv:1409.6301] [INSPIRE].

[115] J. Hisano, D. Kobayashi, N. Mori and E. Senaha, *Effective Interaction of Electroweak-Interacting Dark Matter with Higgs Boson and Its Phenomenology*, *Phys. Lett.* **B 742** (2015) 80 [arXiv:1410.3569] [INSPIRE].

[116] N. Nagata and S. Shirai, *Higgsino Dark Matter in High-Scale Supersymmetry*, *JHEP* **01** (2015) 029 [arXiv:1410.4549] [INSPIRE].

[117] N. Nagata and S. Shirai, *Electroweakly-Interacting Dirac Dark Matter*, *Phys. Rev.* **D 91** (2015) 055035 [arXiv:1411.0752] [INSPIRE].

[118] T. Abe, R. Kitano and R. Sato, *Discrimination of dark matter models in future experiments*, *Phys. Rev.* **D 91** (2015) 095004 [arXiv:1411.1335] [INSPIRE].

JHEP06(2015)097

[119] T. Abe and R. Sato, *Quantum corrections to the spin-independent cross section of the inert doublet dark matter*, *JHEP* **03** (2015) 109 [arXiv:1501.04161] [INSPIRE].

[120] S.M. Boucenna, M.B. Krauss and E. Nardi, *Minimal Asymmetric Dark Matter*, arXiv:1503.01119 [INSPIRE].

[121] M. Kadastik, K. Kannike and M. Raidal, *Matter parity as the origin of scalar Dark Matter*, *Phys. Rev.* **D 81** (2010) 015002 [arXiv:0903.2475] [INSPIRE].

[122] M. Kadastik, K. Kannike and M. Raidal, *Dark Matter as the signal of Grand Unification*, *Phys. Rev.* **D 80** (2009) 085020 [arXiv:0907.1894] [INSPIRE].

[123] M. Frigerio and T. Hambye, *Dark matter stability and unification without supersymmetry*, *Phys. Rev.* **D 81** (2010) 075002 [arXiv:0912.1545] [INSPIRE].

[124] T. Hambye, *On the stability of particle dark matter*, PoS(IDM2010)098 [arXiv:1012.4587] [INSPIRE].

[125] Y. Mambrini, K.A. Olive, J. Quevillon and B. Zaldivar, *Gauge Coupling Unification and Nonequilibrium Thermal Dark Matter*, *Phys. Rev. Lett.* **110** (2013) 241306 [arXiv:1302.4438] [INSPIRE].

[126] L.M. Krauss and F. Wilczek, *Discrete Gauge Symmetry in Continuum Theories*, *Phys. Rev. Lett.* **62** (1989) 1221 [INSPIRE].

[127] L.E. Ibáñez and G.G. Ross, *Discrete gauge symmetry anomalies*, *Phys. Lett.* **B 260** (1991) 291 [INSPIRE].

[128] L.E. Ibáñez and G.G. Ross, *Discrete gauge symmetries and the origin of baryon and lepton number conservation in supersymmetric versions of the standard model*, *Nucl. Phys.* **B 368** (1992) 3 [INSPIRE].

[129] S.P. Martin, *Some simple criteria for gauged R-parity*, *Phys. Rev.* **D 46** (1992) 2769 [hep-ph/9207218] [INSPIRE].

[130] M. De Montigny and M. Masip, *Discrete gauge symmetries in supersymmetric grand unified models*, *Phys. Rev.* **D 49** (1994) 3734 [hep-ph/9309312] [INSPIRE].

[131] Y. Mambrini, N. Nagata, K.A. Olive, J. Quevillon and J. Zheng, *Dark matter and gauge coupling unification in nonsupersymmetric* SO(10) *grand unified models*, *Phys. Rev.* **D 91** (2015) 095010 [arXiv:1502.06929] [INSPIRE].

JHEP06(2015)097